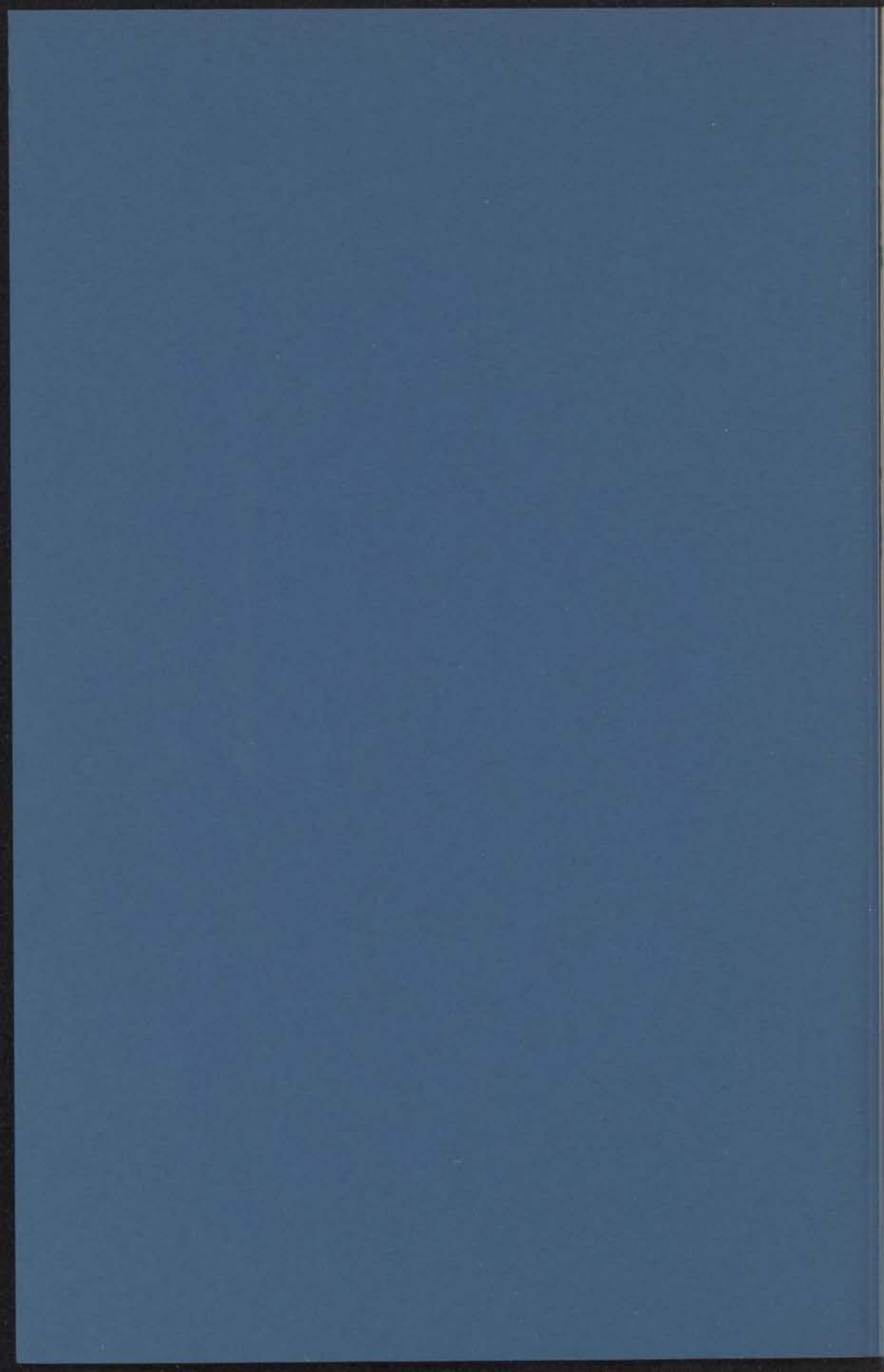


DIFFUSION IN  
BINARY GASEOUS MIXTURES

INSTITUUT-LORENTZ  
voor theoretische natuurkunde  
Nieuwsteeg 16-Leyden-Nederland

R. J. J. VAN HEIJNINGEN



DIFFUSION IN  
BINARY GASEOUS MIXTURES

BINARY GASEOUS MIXTURES

2 OKT. 1967

PROEFSCHRIFT

TEN VERKRIJGING VAN DE GRAAD VAN DOCTOR IN  
DE WISKUNDE EN NATUURWETENSCHAPPEN AAN DE  
RIJSCHE UNIVERSITEIT TE LEIDEN, OP GEBED VAN DE  
RECTOR MAGNIFICUS DR. H. M. VAN DER WOUDE, HOOGLERAAR  
IN DE FACULTEIT DER WISKUNDE, VERDYKT AAN  
VAN EEN COMMISSIE DIE DE SEVAAT IS VERDEELDEN  
OP VRIJDAG 12 OKTOBER 1967 TE 14 UUR

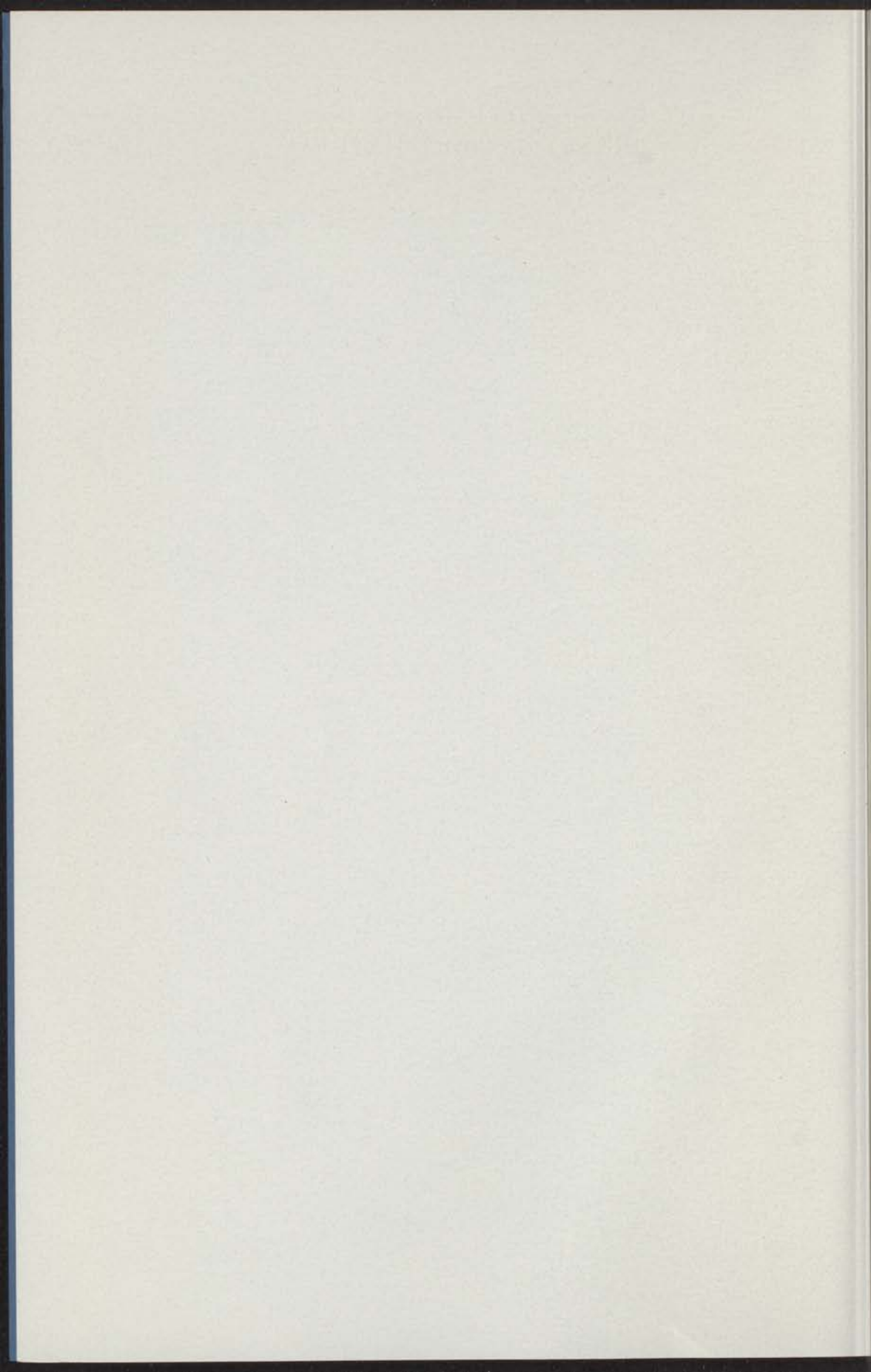
1967

RUDOLPHUS JACOBUS JOZEF VAN REIJNINGEN

OPGEVOERD TE WOLFFENBUTTEL IN 1967

VERKRIJFT BIJ DE  
KONINKLIJKE DRUKKERIJ VAN DE DORPEL VAN  
LEIDEN, 1967

kast dissertaties



# DIFFUSION IN BINARY GASEOUS MIXTURES

PROEFSCHRIFT

TER VERKRIJGING VAN DE GRAAD VAN DOCTOR IN  
DE WISKUNDE EN NATUURWETENSCHAPPEN AAN DE  
RIJKSUNIVERSITEIT TE LEIDEN, OP GEZAG VAN DE  
RECTOR MAGNIFICUS DR. P. MUNTENDAM, HOOGLERAAR  
IN DE FACULTEIT DER GENEESKUNDE, TEN OVERSTAAN  
VAN EEN COMMISSIE UIT DE SENAAAT TE VERDEDIGEN  
OP VRIJDAG 13 OKTOBER 1967 TE 14 UUR

DOOR

RUDOLFUS JACOBUS JOZEF VAN HEIJNINGEN

GEBOREN TE 'S-GRAVENHAGE IN 1938

KONINKLIJKE DRUKKERIJ VAN DE GARDE N.V.

ZALTBOMMEL

# BINARY GASEOUS MIXTURES DIFFUSION IN

PROFESSOR

THE UNIVERSITY OF LEIDEN  
DEPARTMENT OF CHEMISTRY  
IN CONNECTION WITH THE RESEARCHES OF  
THE UNIVERSITY OF LEIDEN  
PROMOTOR: PROF. DR. J. J. M. BEENAKKER

ABOLTES JACOBUS JOSEF VAN HEIJNINGEN

DEPARTMENT OF CHEMISTRY IN LEIDEN

1927

MONISTRIJKE DRUKKERIJ VAN DE GEBR. N.V.

DE WOLFGANG

## CONTENTS

|   |                        |
|---|------------------------|
| INTRODUCTION  | 1                      |
| CHAPTER I - Determination of the diffusion coefficient of the system $N_2-H_2$ as a function of temperature and concentration                 |                        |
| 1. Introduction   | 3                      |
| 2. Apparatus  | 4                      |
| 3. Detection of the concentration   | 6                      |
| 4. Determination of $\nu$ and calculation of $D$  | 7                      |
| 5. Results and consistency tests  | 8                      |
| 6. Comparison with theory and calculation of the potential parameters   | 12                     |
| CHAPTER II - Determination of the diffusion coefficients of binary mixtures of the noble gases as a function of temperature and concentration |                        |
| 1. Introduction   | 17                     |
| 2. Experimental procedure   | 18                     |
| 3. Evaluation of the experimental data  | 19                     |
| a. Determination of $D_{12}$ at $\nu = 0.5$ as a function of temperature  | 19                     |
| b. Determination of $D_{12}$ as a function of concentration   | <i>Aan mijn moeder</i> |
| c. Determination of the potential parameters  | <i>Aan mijn vrouw</i>  |
| 4. Results  |                        |

He did not carry a score of clubs in graded ranks and rigs  
 Or a monstrous bag with a coloured gamp and a clutter of thingummyjigs;  
 He did his work with a long-faced spoon and a weapon he called a cleek,  
 And somehow or other he hit his ball to the middle of this day week.  
 (from Great-Uncle's Golf by Hilton Brown).

Proefster: Prof. Dr. J. J. M. BENNARTS

*Dit werk is een onderdeel van het programma van de Stichting voor Fundamenteel Onderzoek der Materie (F.O.M.) en is mogelijk gemaakt door financiële steun van de Nederlandse Organisatie voor Zuiver Wetenschappelijk Onderzoek (Z.W.O.).*



## CONTENTS

|  |    |
|--|----|
| INTRODUCTION . . . . .   | 1  |
| CHAPTER I - <i>Determination of the diffusion coefficient of the system</i>  |    |
| <i>N<sub>2</sub>-H<sub>2</sub> as a function of temperature and concentration . . . . .</i>  | 3  |
| 1. Introduction . . . . .  | 3  |
| 2. Apparatus . . . . .   | 4  |
| 3. Detection of the concentration . . . . .  | 6  |
| 4. Determination of $\tau$ and calculation of $D$ . . . . .  | 7  |
| 5. Results and consistency tests . . . . .   | 8  |
| 6. Comparison with theory and calculation of the potential parameters . . . . .  | 12 |
| CHAPTER II - <i>Determination of the diffusion coefficients of binary mixtures of the noble gases as a function of temperature and concentration . . . . .</i> |    |
| 1. Introduction . . . . .  | 17 |
| 2. Experimental procedure . . . . .  | 18 |
| 3. Evaluation of the experimental data . . . . .   | 19 |
| a. Determination of $D_{12}$ at $x = 0.5$ as a function of temperature . . . . .   | 19 |
| b. Determination of $D_{12}$ as a function of concentration . . . . .  | 20 |
| c. Determination of the potential parameters . . . . .   | 20 |
| 4. Results . . . . .   | 21 |
| Systems:   |    |
| a. Ne-He . . . . .   | 21 |
| b. Ar-He . . . . .   | 25 |
| c. Kr-He . . . . .   | 25 |
| d. Xe-He . . . . .   | 29 |
| e. Ar-Ne . . . . .   | 29 |
| f. Kr-Ne . . . . .   | 32 |

|  |    |
|--|----|
| g. Xe-Ne . . . . .   | 34 |
| h. Kr-Ar . . . . .   | 34 |
| i. Xe-Ar . . . . .   | 34 |
| j. Xe-Kr . . . . .   | 34 |
| 5. Comparison with other measurements of $D_{12}$ . . . . .  | 38 |
| 6. Discussion of the obtained potential parameters . . . . . | 41 |
| 7. Investigation of the combination rules . . . . .          | 44 |

|  |    |
|--|----|
| SAMENVATTING ( <i>summary in Dutch</i> ) . . . . . | 51 |
|--|----|

|    |   |    |
|----|---|----|
| 1  | Introduction  | 1  |
| 2  | CHAPTER I - Determination of the diffusion coefficient of the system<br>Ne-He as a function of temperature and concentration                      | 2  |
| 3  | 1. Introduction   | 3  |
| 4  | 2. Apparatus  | 4  |
| 5  | 3. Determination of the concentration   | 5  |
| 6  | 4. Determination of $\tau$ and calculation of $D$   | 6  |
| 7  | 5. Results and consistency tests  | 7  |
| 8  | 6. Comparison with theory and calculation of the potential parameters   | 8  |
| 9  | 12. Index   | 12 |
| 10 | CHAPTER II - Determination of the diffusion coefficient of binary mix-<br>tures of the noble gases as a function of temperature and concentration | 17 |
| 11 | 1. Introduction   | 17 |
| 12 | 2. Experimental procedure   | 18 |
| 13 | 3. Evaluation of the experimental data  | 19 |
| 14 | a. Determination of $\tau_{12}$ at $x = 0.5$ as a function of temperature   | 19 |
| 15 | b. Determination of $\tau_{12}$ as a function of concentration  | 20 |
| 16 | c. Determination of the potential parameters  | 20 |
| 17 | 4. Results  | 21 |
| 18 | Systems:  |    |
| 19 | a. Ne-He . . . . .  | 21 |
| 20 | b. Ar-He . . . . .  | 22 |
| 21 | c. Kr-He . . . . .  | 22 |
| 22 | d. Xe-He . . . . .  | 22 |
| 23 | e. Ne-Ar . . . . .  | 22 |
| 24 | f. Ar-Ar . . . . .  | 22 |
| 25 | g. Ne-Kr . . . . .  | 22 |
| 26 | h. Kr-Kr . . . . .  | 22 |
| 27 | i. Ne-Xe . . . . .  | 22 |
| 28 | j. Xe-Xe . . . . .  | 22 |

## INTRODUCTION

One of the ways to obtain information on the interactions between a pair of spherical molecules is the study of the transport properties in a dilute noble gas. In a dilute gas only pair interactions are of importance and for that case a rather rigorous treatment is available in the Chapman-Enskog theory. Transport of a physical quantity is made up from contributions of the individual molecular collisions. So a transport coefficient contains the contributions to the transport of all pairs of colliding molecules, averaged over the impact parameters and the relative kinetic energies. In the Chapman-Enskog theory this procedure results in collision integrals,  $\Omega^{(l,s)}$ , occurring in the expressions for the transport coefficients. From its nature it is clear that a collision integral is not very sensitive to the detailed form of the potential function for a pair of molecules. This is a fortunate circumstance since one can use rather simple potential models in the description of the transport coefficients. For the inverse problem, *i.e.* the derivation of the potential from a transport coefficient, the averaging involved in the collision integrals complicates the situation. Detailed knowledge about the potential can only result from a variation of the distribution of the variables in the collision integrals. The distribution of the impact parameters cannot be influenced experimentally but that of the relative kinetic energies can be changed by varying the temperature. Therefore a transport property will only be a source of significant knowledge about the pair interactions if one can determine accurately the transport coefficient over a large temperature range. This has been verified in viscosity, thermal conductivity and self-diffusion experiments, especially for gases consisting of monatomic molecules.

Extending the study of a transport property to binary **mixtures** of dilute gases one could in general obtain information about the pair interactions that occur between the different species of molecules. Unlike viscosity and thermal conductivity, the diffusion in a mixture refers almost completely to the mixed interactions. Therefore the diffusion coefficient

is one of the best tools to investigate the interactions between unlike molecules.

The present thesis is devoted to the study of the diffusion coefficient of binary gaseous mixtures. Although many investigations on diffusion have been performed during the course of this century, it is surprising that the accuracy has always been rather poor compared to that of viscosity or thermal conductivity experiments. This might be due to the fact that in most cases diffusion measurements are performed in a non-stationary state; systematic errors may easily appear. Primarily it has been our intention to improve the accuracy in diffusion experiments by developing a method which can be shown to be reliable under widely varying conditions. The purpose of these experiments has been to obtain information about the mixed interactions. We have restricted ourselves to the study of gases for which the Chapman-Enskog theory is applicable using simple potential models. This is the case for, *e.g.*, the noble gases. Since the attractive forces between the molecules are more important at lower temperatures the experiments have been performed over a temperature range extending mainly below room temperature. We have carried out an extensive study of the diffusion coefficient at different concentrations of the species composing the mixture. The Chapman-Enskog theory predicts a rather small concentration dependence of the diffusion coefficient. So far this has been verified only in some cases by other investigators.

Chapter I deals with the experimental method used for the determination of diffusion coefficients. The apparatus has been thoroughly tested for nitrogen-hydrogen mixtures over a wide temperature and concentration range. The resulting diffusion coefficients are accurate within 1%. Although  $N_2$ - and  $H_2$ -molecules are not spherical, the experimental data can be brought into agreement with the Chapman-Enskog theory using a potential like the Lennard-Jones (12-6) potential or the (exp-6) potential. The parameters of these potentials belonging to the  $N_2$ - $H_2$  interactions have been derived.

In chapter II diffusion experiments are reported for all binary mixtures composed of the noble gases: He, Ne, Ar, Kr and Xe. For mixtures of widely varying compositions the diffusion coefficients have been determined between 65°K and 400°K. In general rather accurate values of the potential parameters have been derived from the experimental data. We have investigated the combination rules with these values, *i.e.* the relations between the parameters characterizing the pair potentials of like and unlike molecules in a binary mixture.

## DETERMINATION OF THE DIFFUSION COEFFICIENT OF THE SYSTEM $N_2-H_2$ AS A FUNCTION OF TEMPERATURE AND CONCENTRATION

### Synopsis

A method for accurate determination of binary diffusion coefficients as a function of temperature and concentration is described. The apparatus has been thoroughly checked for the system  $N_2-H_2$  between 65° and 300°K. The measured diffusion coefficients are consistent with the Chapman-Enskog theory and allow determination of the intermolecular potential parameters to an accuracy of 1% in  $\epsilon$  and 0.2% in  $\sigma$ . The concentration dependence is also well described by this theory.

1. *Introduction.* According to the Chapman-Enskog theory<sup>1)</sup> the general expression for the diffusion coefficient  $D_{12}$  of a binary gaseous mixture in  $m$ -th approximation is given by

$$[D_{12}]_m = [D_{12}]_1 f_D^{(m)} \quad (1)$$

where

$$[D_{12}]_1 = \frac{3}{8\sqrt{\pi}} \frac{\sqrt{kT/2\mu_{12}}}{\sigma_{12}^2 \Omega_{12}^{(1,1)*}(T_{12}^*)} \frac{1}{n} \quad (2)$$

or in terms of the pressure

$$[D_{12}]_1 = \frac{3}{8\sqrt{\pi}} \frac{\sqrt{k^3 T^3 / 2\mu_{12}}}{\sigma_{12}^2 \Omega_{12}^{(1,1)*}(T_{12}^*)} \frac{1}{p} \quad (3)$$

$f_D^{(m)}$  takes into account the contribution of higher terms in the Sonine expansion. In these expressions  $p$ ,  $n$ ,  $T$  and  $\mu$  denote pressure, density, temperature and reduced mass respectively;  $k$  is Boltzmann's constant; the subscripts 1 and 2 refer to molecules of species 1 and 2. The intermolecular potential model, in which the depth of the well is given by  $\epsilon$  and the minimum separation for zero energy by  $\sigma$ , enters eq. (2) or (3) through  $\sigma_{12}$  and  $\Omega_{12}^{(1,1)*}(T_{12}^*)$ , with  $T_{12}^* = kT/\epsilon_{12}$ .  $\Omega^{(1,1)*}$  is the diffusion collision integral, reduced in the usual way<sup>2)</sup>. As the right hand side of eq. (3) depends only on the properties of mixed interaction, the first Chapman-Enskog approximation of  $D_{12}$  (in which  $f_D = 1$ ) is very

suitable for getting information on  $\epsilon_{12}$  and  $\sigma_{12}$ . This is in contrast to *e.g.*, the other transport properties since these contain the parameters of the pure components as well. To be able to determine  $\epsilon_{12}$  and  $\sigma_{12}$  from the experimental values of  $D$  one needs accurate measurements over a large temperature range because  $\Omega^{(1,1)*}$  depends only slightly on temperature. Furthermore one has to derive  $[D]_1$  from the measured values of  $D$ . The correction factor  $f_D$  due to the higher approximations of  $D$  differs only a few percent from unity. It is, however, dependent on concentration. For this reason one has to measure  $D$  as a function of concentration too.

We will describe a method that gives the desired accuracy over a large enough temperature and concentration range.

**2. Apparatus.** A schematic diagram of the diffusion cell that is placed in a cryostat is shown in fig. 1. The apparatus consists of two cylindrical brass chambers, closed at both ends by brass flanges with indium "o" ring seals. The chambers are connected by an interchangeable stainless

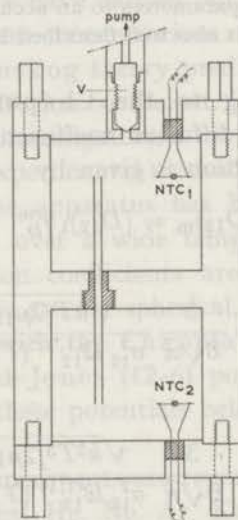


Fig. 1. Apparatus

steel capillary that is screwed with a teflon tape seal into the separating wall. The volumes of the chambers are 100 cm<sup>3</sup> each; the capillaries vary from 2.5 to 10 cm in length and from 0.045 to 0.137 cm in radius. The cell is connected with the filling system and an oil manometer by a German silver tube, which can be closed by a stainless steel precision needle valve  $V$ , operated from the top of the cryostat.

At the start of an experiment the apparatus is filled with a mixture. The

needle valve  $V$  is closed and the gas above  $V$  is exchanged for some gas with a different composition. Then the concentration in the upper vessel is changed about 5% by opening the needle valve for some time. After  $V$  is closed we wait a few minutes for transient effects to die out and then the difference in concentration between the upper and lower chamber is registered. A diffusion measurement consists thus of the determination of a concentration-time diagram.

The concentration is continuously measured by thermistors, N.T.C.<sub>1</sub> and N.T.C.<sub>2</sub>, using the dependence of the thermal conductivity of a mixture on composition. At low temperatures we used thermistors from Keystone Carbon Company (St. Marys, Pennsylvania), type L 0904-730 TO<sup>3</sup>, while at room temperature we used thermistors from Standard Telephones and Cables Ltd. (Footscray, Sidcup, Kent), type R 13-1 PK, the glass vacuum covers of which were removed. The thermistors are mounted on the upper and lower flange of the cell using "electrovac" seals (Vienna, Austria), type H 113 A9, for the connecting wires. The variation of the resistances of the thermistors in the upper and lower chamber is differentially determined in a Wheatstone bridge with a recording millivoltmeter.

The concentration detection method using thermistors requires very good temperature stability as one can see from the following example. In a mixture of 50% N<sub>2</sub>-H<sub>2</sub> we initially set up a concentration gradient of say at most 5%. As a result the temperature difference between thermistor and walls, which was in most cases not more than 2°C, will change by about 0.1°C. For accurate diffusion measurements one requires a sensitivity of  $2 \cdot 10^{-3}$  in the concentration determination. This means a temperature stability within  $2 \cdot 10^{-4}$ °C over the time that a diffusion run takes place. At low temperatures this stability is for the greater part achieved in the following way. We have surrounded the apparatus (diameter 6.5 cm) by a brass jacket (diameter 8.5 cm), closed at the bottom. The whole system is placed in a wide cryostat (diameter 14 cm) that is filled with a boiling liquid. A heater at the bottom of the cryostat creates a fine stream of vapour bubbles around the apparatus. Since the jacket screens the cell from a vigorous streaming of the cooling liquid, the temperature in the neighbourhood of the cell is stabilized at a value corresponding to the hydrostatic pressure.

At room temperature we used a commercial water thermostat, constant to  $\pm 0.01$ °C, while the same jacket, filled with oil, served as a buffer. The remaining instability is canceled by using thermistors with equal temperature coefficients in the Wheatstone bridge circuit.

The measuring temperatures are derived from the vapour pressure of the cooling liquids, applying a correction for the height of the liquid column above the centre of the cell.

The gases we have used are from laboratory stock and have a purity better than 99.9%. This has been checked in a thermal diffusion apparatus with a resolution of about 0.05%.<sup>4)</sup>

3. *Detection of the concentration.* The concentration difference in the chambers will decrease to zero according to the relation

$$x_t^u - x_\infty = (x_0^u - x_\infty) e^{-t/\tau} \quad (4)$$

where

$$\frac{1}{\tau} = D_{12} \frac{A}{l_{\text{cap}}} \left( \frac{1}{V^u} + \frac{1}{V^l} \right) (1 + \zeta). \quad (5)$$

Here  $x$  denotes the concentration,  $V$  is the volume of a chamber and  $l_{\text{cap}}$  and  $A$  are the capillary length and cross sectional area. The superscripts  $u$  and  $l$  denote the upper and lower chamber, while the subscripts  $t$ ,  $0$  and  $\infty$  describe different times.  $\zeta$  is a correction term that will be discussed in section 4. Using an equation similar to eq. (4) for the lower chamber we can write for the difference in concentration  $\Delta x$ , between both chambers

$$(\Delta x)_t = x_t^u - x_t^l = (\Delta x)_0 e^{-t/\tau}. \quad (6)$$

To determine  $\tau$  we have to measure the variation of  $\Delta x$  as a function of time. Since the concentration of a mixture is not proportional to, *i.a.*, its thermal conductivity, the recorded signal can be expected to be nonlinear in the concentration. We will now show that due to the symmetry in the apparatus nonlinear effects cancel. Expanding the recorded signal  $E^u$  for the upper chamber alone, we obtain

$$E_t^u - E_\infty = (x_t^u - x_\infty) \left( \frac{dE^u}{dx} \right)_{x=x_\infty} + \frac{1}{2} (x_t^u - x_\infty)^2 \left( \frac{d^2E^u}{dx^2} \right)_{x=x_\infty}. \quad (7)$$

If the dependence of  $E$  on  $x$  is the same for both thermistors one gets on writing eq. (7) for both chambers and subtracting

$$E_t^u - E_t^l = (x_t^u - x_t^l) \left( \frac{dE}{dx} \right)_{x=x_\infty} + \frac{1}{2} (x_0^u - x_0^l) (x_0^u + x_0^l - 2x_\infty) e^{-2t/\tau} \left( \frac{d^2E}{dx^2} \right)_{x=x_\infty}. \quad (8)$$

If the chambers are equal in volume,  $x_0^u + x_0^l - 2x_\infty = 0$ , and hence the nonlinear term disappears. The difference in  $dE/dx$  between the thermistors under the same surrounding conditions has been kept always smaller than 5% while the volumes were equal within 0.5%. This means that no corrections for nonlinearity have to be applied in this apparatus.



4. *Determination of  $\tau$  and calculation of  $D$ .* From the slope of a  $\log |(\Delta x)_t|$  vs. time plot (see eq. (6)) one could determine  $\tau$  graphically. This method, however, has several drawbacks. The asymptotic value is not known since, due to the slight inequality of the thermistors, the zero point is shifted after a run. If one tries to estimate the value of the asymptote from the experimental curve, there is a tendency to give too much weight to the end of the curve. This can prove awkward because a constant temperature drift, that has a negligible effect at the beginning of the curve, is important at its asymptotic value. For this reason we prefer the following procedure.

We take as reference the initial situation. From eq. (6) we obtain the following expression:

$$(\Delta x)_0 - (\Delta x)_t = (\Delta x)_0 (1 - e^{-t/\tau}). \quad (9)$$

When we plot the experimental data as  $\log |(\Delta x)_0 - (\Delta x)_t|$  vs.  $\log t$  we get a curve the form of which is independent of both  $\tau$  and  $(\Delta x)_0$ , since  $\log(1 - e^{-t/\tau})$  is only a function of the ratio  $t/\tau$ . We compare the curve so obtained with a plot of  $\log(1 - e^{-t})$  vs.  $\log t$ . The shape of these curves should then be identical. From the shifts along the axis, necessary to make

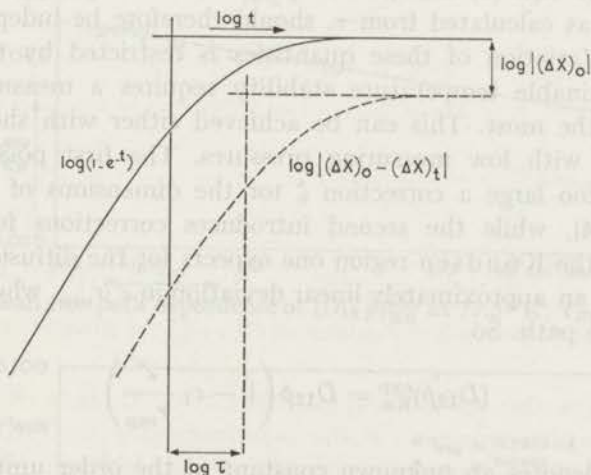


Fig. 2. Determination of  $\tau$ .

both curves coincide, one obtains the values of  $\log \tau$  and  $\log |(\Delta x)_0|$  (see fig. 2). Not only does one use in this way the total experimental information but this method also shows accurately that nonexponential perturbation in a diffusion run does not occur.

With eq. (5) one can calculate  $D$  from  $\tau$ . The uncertainty in the dimensions of the apparatus never exceeds 0.2%. The derivation of eqs. (4) and (5) is made for an idealized situation ( $\zeta = 0$ ). Under experimental conditions one has to take into account the following effects:

a) The volume of the capillary is not negligible compared to the volumes of the chambers<sup>5)</sup>.

b) The concentration gradient in the capillary is not linear<sup>6)</sup>.

c) End effects give rise to a difference between the geometrical and the effective length of the capillary<sup>7) 8)</sup>. In our case the corrections for a) and b) together are always smaller than 0.5%, while the correction for c) varies from 0.7 to 4.3%. We do not apply corrections for the variation of  $D$  with concentration during an experiment, as these turn out to be negligible.<sup>6)</sup> Furthermore the influence of a concentration gradient in the chambers can be neglected.<sup>5)</sup> Transient effects are avoided by waiting some time<sup>9)</sup>. For a full discussion of these effects we refer to the original papers mentioned above.

5. *Results and consistency tests.* For reliable results it is obvious that the measured diffusion curves should be exponential (see section 4). Since also most disturbances will die out exponentially with nearly the same time constant, this is, however, not sufficient; other consistency tests are necessary.

According to eqs. (3) and (5)  $\tau$  is proportional to  $\phi$ ,  $l_{\text{cap}}$  and  $1/A$ . The value of  $D\phi$ , as calculated from  $\tau$ , should therefore be independent of  $\phi$ ,  $l_{\text{cap}}$  and  $A$ . Variation of these quantities is restricted by the condition that the attainable temperature stability requires a measuring time of one hour at the most. This can be achieved either with short and wide capillaries or with low measuring pressures. The first possibility leads, however, to too large a correction  $\zeta$  for the dimensions of the capillary (see section 4), while the second introduces corrections for Knudsen effects. Near the Knudsen region one expects for the diffusion coefficient as measured, an approximately linear deviation in  $\ell/r_{\text{cap}}$ , where  $\ell$  signifies the mean free path. So

$$(D_{12}\phi)_{\text{Kn}}^{\text{exp}} = D_{12}\phi \left( 1 - c_1 \frac{\ell}{r_{\text{cap}}} \right) \quad (10)$$

in which  $c_1$  denotes an unknown constant of the order unity, depending on the surface of the capillary. Since  $\ell$  is proportional to  $T/\phi$ , eq. (10) can be written as

$$(D_{12}\phi)_{\text{Kn}}^{\text{exp}} = D_{12}\phi \left( 1 - c_2 \frac{T}{\phi r_{\text{cap}}} \right) \quad (11)$$

hence the plot of  $(D_{12}\phi)_{\text{Kn}}^{\text{exp}}$  vs.  $1/\phi r_{\text{cap}}$  is expected to show a straight line at constant temperature. In figs. 3, 4, 5, 6 and 7, where every symbol signifies a value averaged over 3 to 5 runs, the validity of eq. (11) is shown. Only at high values of  $T/\phi r_{\text{cap}}$  eq. (11) does no longer hold (see fig. 7). The values of  $D_{12}\phi$  are obtained by extrapolation to  $1/\phi r_{\text{cap}} = 0$ . This

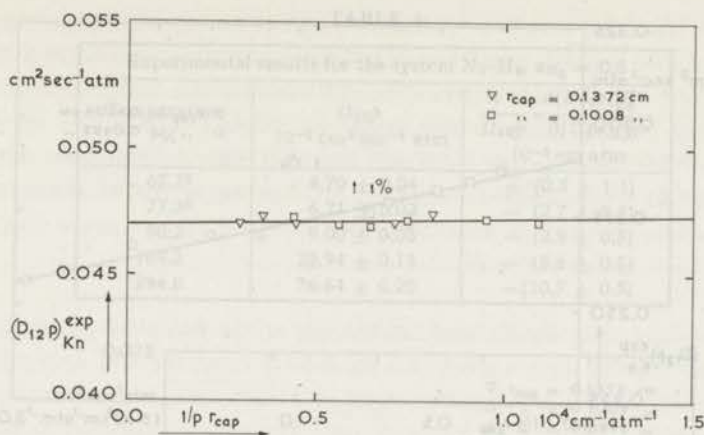


Fig. 3. Mean free path dependence of  $(D_{12} p)_{Kn}^{exp}$  at  $65.25^\circ K$ ;  $x_{H_2} = 0.5$ .

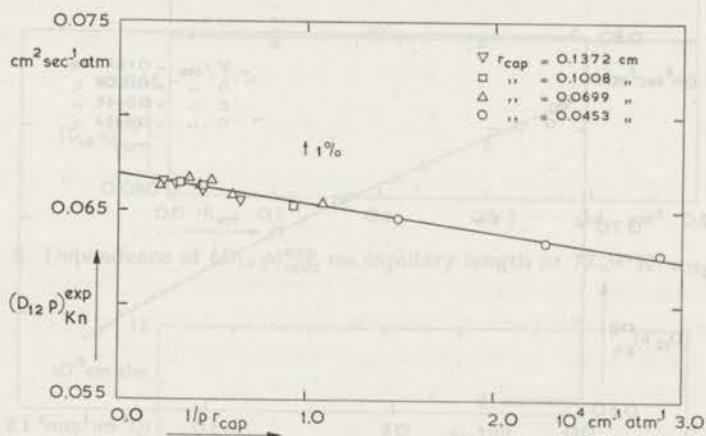


Fig. 4. Mean free path dependence of  $(D_{12} p)_{Kn}^{exp}$  at  $77.35^\circ K$ ;  $x_{H_2} = 0.5$ .

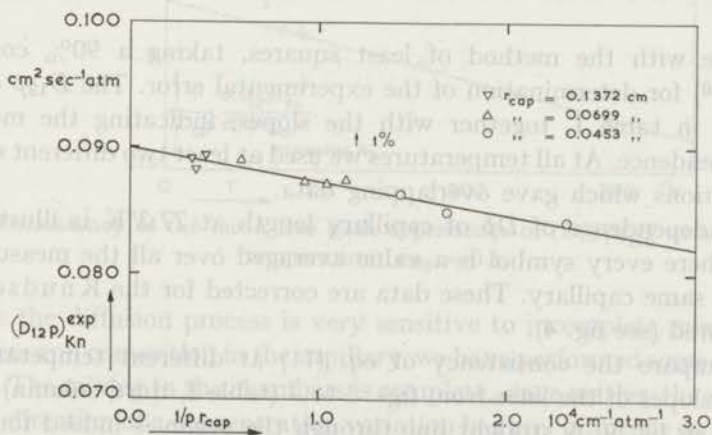


Fig. 5. Mean free path dependence of  $(D_{12} p)_{Kn}^{exp}$  at  $90.2^\circ K$ ;  $x_{H_2} = 0.5$ .

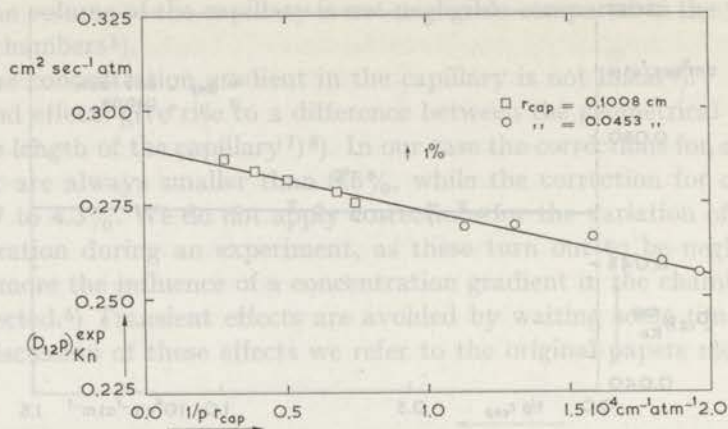


Fig. 6. Mean free path dependence of  $(D_{12}p)_{Kn}^{exp}$  at 169.3°K;  $x_{H_2} = 0.5$ .

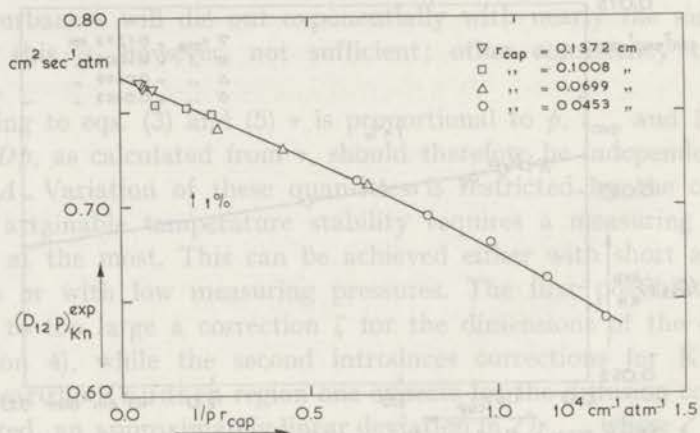


Fig. 7. Mean free path dependence of  $(D_{12}p)_{Kn}^{exp}$  at 294.8°K;  $x_{H_2} = 0.5$ .

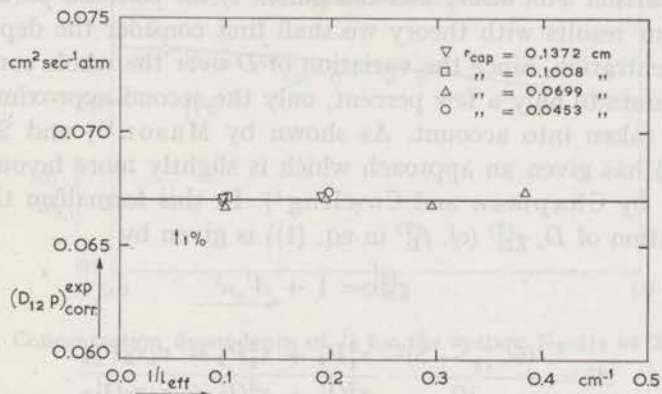
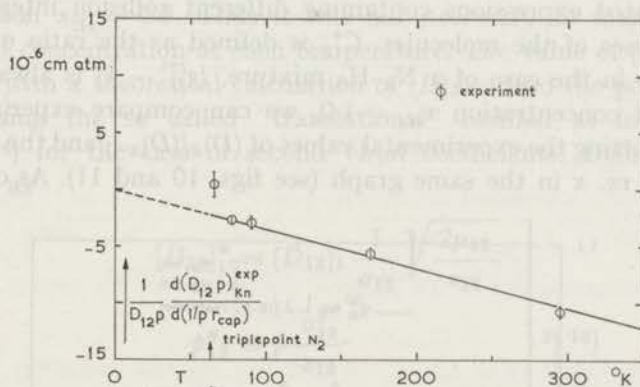
was done with the method of least squares, taking a 90% confidence interval<sup>10</sup>) for determination of the experimental error. The  $D_{12}p$  data are collected in table I, together with the slopes, indicating the mean free path dependence. At all temperatures we used at least two different capillary cross sections which gave overlapping data.

The independence of  $Dp$  of capillary length at 77.3°K is illustrated in fig. 8, where every symbol is a value averaged over all the measurements with the same capillary. These data are corrected for the Knudsen effect as measured (see fig. 4).

To compare the consistency of eq. (11) at different temperatures we plot the slopes of the lines from figs. 3 to 7 (table I, third column) vs. temperature in fig. 9. A straight line through the origin is indeed found. The deviation of the value at 65°K will be considered in the next section.

TABLE I

| Experimental results for the system $N_2-H_2$ , $x_{H_2} = 0.5$ |  |   |
|---|--|---|
| Temperature<br>°K   | $D_{12}p$<br>$10^{-2} \text{ cm}^2 \text{ sec}^{-1} \text{ atm}$ | $1 \frac{d(D_{12}p)_{Kn}^{exp}}{D_{12}p \ d(1/pr_{cap})}$ |
|   |  | $10^{-6} \text{ cm atm}$                                  |
| 65.2 <sup>b</sup>   | $4.70 \pm 0.04$  | + (0.5 ± 1.1)   |
| 77.3 <sup>b</sup>   | $6.71 \pm 0.02$  | - (2.7 ± 0.3)   |
| 90.2  | $9.00 \pm 0.05$  | - (2.9 ± 0.5)   |
| 169.3   | $28.94 \pm 0.15$   | - (5.6 ± 0.5)   |
| 294.8   | $76.64 \pm 0.20$   | - (10.7 ± 0.5)  |

Fig. 8. Dependence of  $(D_{12}p)_{corr}^{exp}$  on capillary length at  $77.35^\circ K$ ;  $x_{H_2} = 0.5$ .Fig. 9. Consistency of the mean free path dependence of  $(D_{12}p)_{Kn}^{exp}$  as a function of temperature;  $x_{H_2} = 0.5$ .

Since the diffusion process is very sensitive to incomplete mixing in the chambers and convection in the capillary, we have performed some additional checks. The mixing in the chambers is complete, since neither the magnitude nor the direction of a concentration variation has any influence on the values obtained for  $\tau$ . This is due mainly to the absence of dead space and shows

furthermore that the diffusion resistance in the cell is negligible compared to the resistance of the capillary. Convection in the chambers, which is caused mainly by the thermistors, might disturb the diffusion process in the capillary. Such a disturbance does not occur because the results are independent of the heating current through the thermistors. The heat input of the low temperature thermistors has been varied from 1 to 15 milliwatt, while the much smaller ones for room temperature have been checked with 0.1 and 0.5 mW.

6. *Comparison with theory and calculation of the potential parameters.* To compare our results with theory we shall first consider the dependence of  $D$  on concentration. Since the variation of  $D$  over the whole concentration range amounts to only a few percent, only the second approximation of  $D$  has to be taken into account. As shown by Mason<sup>11)</sup> and Saxena<sup>12)</sup>, Kihara<sup>13)</sup> has given an approach which is slightly more favourable than that given by Chapman and Cowling<sup>1)</sup>. In this formalism the second approximation of  $D$ ,  $g_D^{(2)}$  (cf.  $f_D^{(2)}$  in eq. (1)) is given by

$$g_D^{(2)} = 1 + A' \quad (12)$$

where

$$A' = \frac{(6C_{12}^* - 5)^2}{10} \frac{x_1^2 P_1 + x_2^2 P_2 + x_1 x_2 P_{12}}{x_1^2 Q_1' + x_2^2 Q_2' + x_1 x_2 Q_{12}'} \quad (13)$$

The quantities  $P$  and  $Q'$  are the same as those defined by Mason<sup>11)</sup>. They are complicated expressions containing different collision integrals  $\Omega^{(1,s)*}$  and the masses of the molecules.  $C_{12}^*$  is defined as the ratio of  $\Omega_{12}^{(1,2)*}$  to  $\Omega_{12}^{(1,1)*}$ . Since in the case of a  $N_2$ - $H_2$  mixture,  $(g_D^{(2)} - 1)$  is always smaller than  $10^{-4}$  at concentration  $x_{H_2} = 1.0$ , we can compare experiment with theory by plotting the experimental values of  $(D)_x / (D)_{x=1}$  and the theoretical function  $g_D^{(2)}$  vs.  $x$  in the same graph (see figs. 10 and 11). As one can see

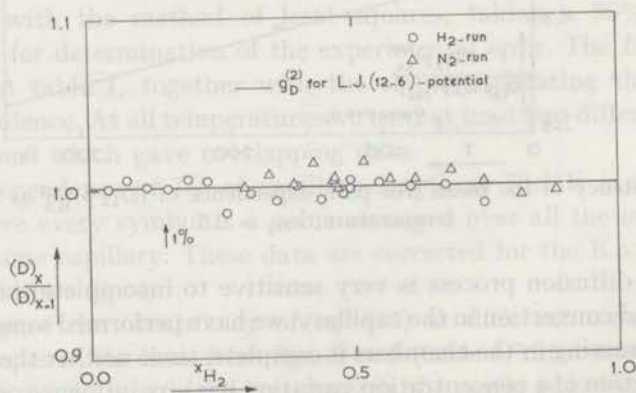


Fig. 10. Concentration dependence of  $D$  for the system  $N_2$ - $H_2$  at  $77.35^\circ K$ .

good agreement between theory and experiment is found. At 294.8°K we get the best fit of our data for an exp-6 potential, with  $\alpha = 14$ , but within the accuracy of the measurements other potential models: exp-6 ( $\alpha = 12, 13$  and 15), Lennard-Jones (12-6) are also possible. At 77.3°K the same good agreement with theory is found but since the concentration dependence is very small, there is no special potential model preferable. This good

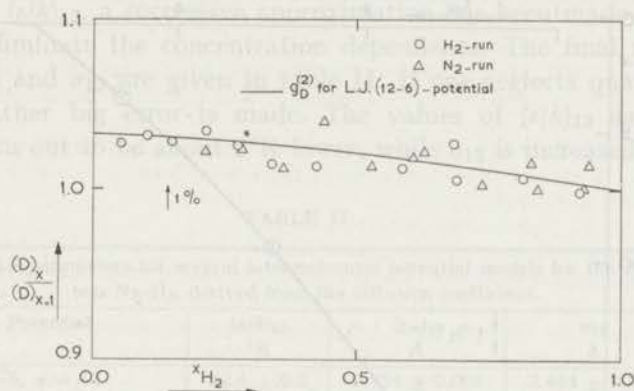


Fig. 11. Concentration dependence of  $D$  for the system  $N_2-H_2$  at 294.8°K.

agreement allows us to calculate  $(D)_{x=1}^{\text{exp}}$ , for concentration  $x_{H_2} = 1.0$ , from the measured values of  $(D)_{x=0.5}^{\text{exp}}$  using a theoretical estimate of  $g_D^{(2)}$  at concentration  $x_{H_2} = 0.5$ . Thus it was not necessary to measure  $D$  as a function of concentration at each temperature. The value of  $(D)_{x=1}^{\text{exp}}$  is now compared with a theoretical calculation of  $[D]_1$  to find the potential parameters, using the so called "translational" method as introduced by Keesom<sup>14</sup> for the case of second virial coefficients. Defining reduced quantities as

$$\left. \begin{aligned} [D_{12}]_1^* &\equiv [D_{12}]_1 \frac{1}{\sigma_{12}} \sqrt{\frac{2\mu_{12}}{\epsilon_{12}}} \\ \hat{p}_{12}^* &\equiv \hat{p} \frac{\sigma_{12}^3}{\epsilon_{12}} \\ T_{12}^* &\equiv T \frac{k}{\epsilon_{12}} \end{aligned} \right\} \text{2) 15)} \quad (14)$$

we get using eq. (3)

$$\frac{[D_{12}]_1^* \hat{p}_{12}^*}{\sqrt{T_{12}^{*3}}} = \frac{[D_{12}]_1 \hat{p}}{\sqrt{k^3 T^3 / 2\mu_{12}}} \sigma_{12}^2 = \frac{3/8\sqrt{\pi}}{\Omega_{12}^{(1,1)*}(T_{12}^*)} \quad (15)$$

We plot the experimental results as  $\log \{(D_{12})_{x=1}^{\text{exp}} \hat{p} / \sqrt{k^3 T^3 / 2\mu_{12}}\}$  vs.  $\log T$

which curve should have the same shape as the theoretical curve of  $\log \{ [D_{12}]_1^* \rho_{12}^* / \sqrt{T_{12}^{*3}} \}$  vs.  $\log T_{12}^*$ , the latter curve being determined by  $\Omega_{12}^{(1,1)*}(T_{12}^*)$ . The shifts in the direction of the abscissa and ordinate determine  $\log(\epsilon/k)_{12}$  and  $\log \sigma_{12}^2$  respectively. This procedure (see fig. 12) is followed using  $\Omega$ -data for the Lennard-Jones (12-6) potential and

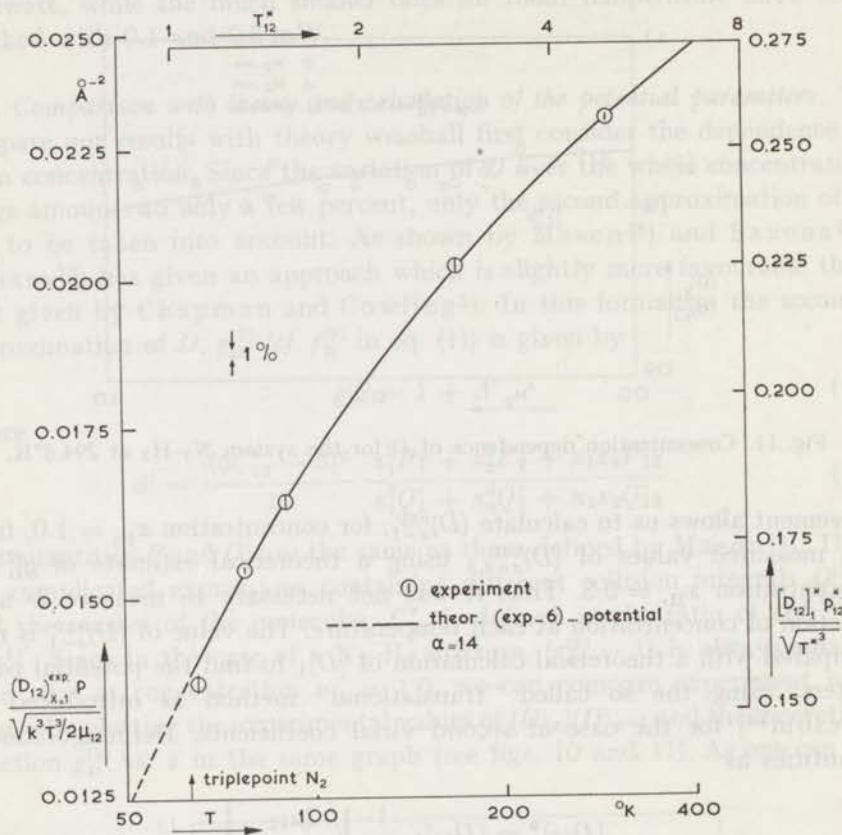


Fig. 12. Determination of the potential parameters for the system  $N_2-H_2$ .

the exp-6 potential ( $\alpha = 12, 13, 14$  and  $15$ ). As the quantum parameter,  $A^* = h/\sigma_{12} \sqrt{2\mu_{12}\epsilon_{12}}$  for the system  $N_2-H_2$  amounts to 0.89, quantum mechanical effects cannot be neglected in the temperature range where  $T^* < 5$ . We have obtained the quantum mechanically calculated values of  $\Omega^{(1,1)*}$  for the Lennard-Jones (12-6) potential by interpolation of the tables from Munn *et al.*<sup>16</sup>). For other potential models no quantum mechanical calculations of  $\Omega^{(1,1)*}$  have been performed. Since the data of Munn *et al.* for the classical case ( $A^* = 0$ ) deviate not more than 2.5% from those at  $A^* = 0.89$ , for  $T^* > 1$ , we have calculated the  $\Omega^{(1,1)*}$  data



for the other potential models by assuming, that to a good approximation

$$(\Omega_{A^*=0.89}^{(1,1)^*})_{\text{exp-6}} = \left( \frac{\Omega_{A^*=0.89}^{(1,1)^*}}{\Omega_{A^*=0}^{(1,1)^*}} \right)_{\text{L.J.}(12-6)} (\Omega_{A^*=0}^{(1,1)^*})_{\text{exp-6}} \quad (16)$$

In this way the classical  $\Omega^{(1,1)^*}$ -data for the exp-6 potential, as tabulated by Mason<sup>17)</sup> have been corrected for quantum effects.

Since  $g_D^{(2)}$  is mainly determined by  $C_{12}^*(T_{12}^*)$ , which depends strongly on the choice of  $(\epsilon/k)_{12}$ , a successive approximation has been made for  $(\epsilon/k)_{12}$  and  $\sigma_{12}$  to eliminate the concentration dependence. The final results for  $(\epsilon/k)_{12}$ ,  $(r_m)_{12}$  and  $\sigma_{12}$  are given in table II. If one neglects quantum corrections a rather big error is made. The values of  $(\epsilon/k)_{12}$  as obtained classically turn out to be about 5°K lower, while  $\sigma_{12}$  is increased by about 0.02 Å.

TABLE II

| Potential parameters for several intermolecular potential models for the system N <sub>2</sub> -H <sub>2</sub> , derived from the diffusion coefficient. |                           |                   |                    |
|--|---------------------------|-------------------|--------------------|
| Potential  | $(\epsilon/k)_{12}$<br>°K | $(r_m)_{12}$<br>Å | $\sigma_{12}$<br>Å |
| Exp -6, $\alpha = 12$  | 50.4 ± 0.5                | 3.954 ± 0.008     | 3.464 ± 0.008      |
| " $\alpha = 13$  | 56.0 ± 0.3                | 3.835 ± 0.005     | 3.387 ± 0.005      |
| " $\alpha = 14$  | 60.8 ± 0.3                | 3.747 ± 0.005     | 3.331 ± 0.005      |
| " $\alpha = 15$  | 65.2 ± 0.3                | 3.678 ± 0.005     | 3.289 ± 0.005      |
| Lennard-Jones (12-6)   | 62.9 ± 0.5                | 3.687 ± 0.008     | 3.285 ± 0.008      |

As in the case of the concentration dependence the experimental results for  $[D_{12}]_1$  fit the theory for all of the investigated potential models, but the best agreement is obtained for an exp-6 potential,  $\alpha = 13$  or 14.

A comparison with the results for  $(\epsilon/k)_{12}$  and  $\sigma_{12}$ , as obtained from combination rules<sup>2)</sup>, can be made for the Lennard-Jones (12-6) potential parameters. From the values of  $\epsilon/k$  and  $\sigma$  for the pure gases N<sub>2</sub> and H<sub>2</sub>, as determined from the second virial coefficient measurements of Michels *et al.*<sup>18)19)</sup> we get

$$(\epsilon/k)_{12} = \sqrt{(\epsilon/k)_{11} (\epsilon/k)_{22}} = 59.3^\circ\text{K}$$

$$\sigma_{12} = \frac{\sigma_{11} + \sigma_{22}}{2} = 3.31 \text{ \AA}.$$

Although the combination rules are not very well founded, the agreement with our results is quite good.

In the preceding considerations we have omitted the low value of  $D$  at  $T = 65^\circ\text{K}$  since there was some uncertainty in this experimental value. At this very low temperature one gets easily adsorption of N<sub>2</sub>, increasing with increasing pressure. Also this is probably the reason why the value of  $(1/D_{12}p)\{[d(D_{12}p)_{\text{Kn}}^{\text{exp}}]/[d(1/pr_{\text{cap}})]\}$  at 65°K deviates so much from the trend of the data at higher temperatures (see fig. 9).

REFERENCES

- 1) Chapman, S. and Cowling, T. G., The Mathematical Theory of Non-Uniform Gases (Cambridge University Press, New York, 1952).
- 2) Hirschfelder, J. O., Curtiss, C. F. and Bird, R. B., The Molecular Theory of Gases and Liquids (John Wiley and Sons, Inc., New York, 1954).
- 3) Sachse, H. B., Temperature - Its Measurement and Control in Science and Industry, Vol. 3, Part 2, **30**. (Reinhold Publishing Corp., New York, 1962).
- 4) Van Ee, H., Thesis Leiden (1966).  
Van Ee, H., Knaap, H. F.P. and Beenakker, J. J. M., Physica (to be published).
- 5) Ney, E. P. and Armistead, F. C., Phys. Rev. **71** (1947) 14.
- 6) Paul, R., Phys. Fluids **3** (1960) 905.
- 7) Lord Rayleigh, Theory of Sound (MacMillan and Co., London, 1878), Vol. II, p. 291.
- 8) Maxwell, J. C., Electricity and Magnetism (Oxford University Press, London, 1891), Vol. I, p. 434.
- 9) Loeb, J., Kinetic Theory of Gases (McGraw-Hill Book Company, Inc., New York, 1934), p. 268.
- 10) Bowker, A. H. and Lieberman, G. J., Engineering Statistics (Prentice-Hall, Inc., Englewood Cliffs, N.J., 1959).
- 11) Mason, E. A., J. chem. Phys. **27** (1957) 75; 782.
- 12) Saxena, S. C., J. phys. Soc. Japan **11** (1956) 367.
- 13) Kihara, T., Imperfect Gases (Asakura Bookstore, Tokyo, 1949). Rev. mod. Phys. **25** (1953) 831.
- 14) Keesom, W. H., Commun. Phys. Lab. Leiden, Suppl. No. 25 (1912).
- 15) Carswell, A. I. and Stryland, J. C., Canad. J. Phys. **41** (1963) 708.
- 16) Munn, R. J., Smith, F. J., Mason, E. A. and Monchick, L., J. chem. Phys. **42** (1965) 537.
- 17) Mason, E. A., J. chem. Phys. **22** (1954) 169.
- 18) Michels, A. and Goudekot, M., Physica **8** (1941) 347.
- 19) Michels, A., Wouters, H. and De Boer, J., Physica **1** (1934) 587.

As in the case of the concentration dependence the experimental results for  $\lambda_{\text{eff}}$  in the theory for all of the investigated potential models for the best agreement is obtained for an exp-6 potential  $\epsilon = 12$  or 14. A comparison with the results for  $\lambda_{\text{eff}}$  and  $\lambda_{\text{eff}}$  as obtained from the experimental data can be made for the Lennard-Jones (12-6) potential parameter. From the values of  $\lambda_{\text{eff}}$  and  $\lambda_{\text{eff}}$  for the pure gases  $N_2$  and  $H_2$  as determined from the second virial coefficient measurements of Michels

Fig. 12. Determination of the quantum parameter  $\lambda_{\text{eff}}$  for the system  $N_2-H_2$ .

$$\lambda_{\text{eff}} = \sqrt{\frac{2m}{3kT}} \left( \frac{1}{\lambda_{\text{eff}}} + \frac{1}{\lambda_{\text{eff}}} \right) = 27.3 \text{ \AA}$$

the exp-6 potential  $\epsilon = 12, 13, 14$  and 15). As the quantum parameter,  $\lambda_{\text{eff}}$  is defined by  $\lambda_{\text{eff}} = \sqrt{\frac{2m}{3kT}} \left( \frac{1}{\lambda_{\text{eff}}} + \frac{1}{\lambda_{\text{eff}}} \right)$ . Although the mechanical effects cannot be neglected in determining  $\lambda_{\text{eff}}$  in the present investigation, we have omitted the mechanical effects in the present investigation. At this point there was a discrepancy in the experimental values of  $\lambda_{\text{eff}}$  for  $N_2$  and  $H_2$  which was caused by a difference in the way with which the parameter  $\lambda_{\text{eff}}$  is defined. In this study we have used the definition of  $\lambda_{\text{eff}}$  as given in the literature. The values of  $\lambda_{\text{eff}}$  for  $N_2$  and  $H_2$  are given in Table I. It is seen from these values that the quantum parameter  $\lambda_{\text{eff}}$  is about 10% larger for  $N_2$  than for  $H_2$ .

## DETERMINATION OF THE DIFFUSION COEFFICIENTS OF BINARY MIXTURES OF THE NOBLE GASES AS A FUNCTION OF TEMPERATURE AND CONCENTRATION

### Synopsis

The diffusion coefficients,  $D_{12}$ , of the ten binary mixtures of the noble gases: He, Ne, Ar, Kr and Xe, have been measured as a function of temperature and concentration using a method similar to the one described in chapter I. In general the diffusion coefficients are well described by the Chapman-Enskog theory with the Lennard-Jones (12-6) potential or the (exp-6) potential. From the experimental data the potential parameters,  $\epsilon_{ij}$  and  $\sigma_{ij}$ , of the mixed interaction have been calculated. Some combination rules connecting the mixed parameters with those of the pure components have been tested. Only the rule  $\epsilon_{ij}\sigma_{ij}^6 = (\epsilon_{ii}\sigma_{ii}^6\epsilon_{jj}\sigma_{jj}^6)^{1/2}$  agrees with the experiments.

1. *Introduction.* In chapter I<sup>1)</sup> we have described a method for an accurate determination of the diffusion coefficients for binary gaseous mixtures over a wide range of temperature and concentration. Such measurements give rather direct information on the potential between a pair of unlike molecules. This can be seen from the Chapman-Enskog expression<sup>2)3)</sup> for the binary diffusion coefficient,  $D_{12}$  ( $m^{\text{th}}$  order):

$$[D_{12}]_m = [D_{12}]_1 f_D^{(m)}(x) \quad (1)$$

$$[D_{12}]_1 = \frac{3}{8\sqrt{\pi}} \frac{\sqrt{k^3 T^3 / 2\mu_{12}}}{\sigma_{12}^2 \Omega_{12}^{(1,1)*}(T_{12}^*)} \frac{1}{p} \quad (2)$$

where

$k$  = Boltzmann's constant

$T$  = temperature

$\mu$  = reduced mass

$p$  = pressure

$\Omega^{(1,1)*}(T^*)$  = reduced collision integral<sup>3)</sup>

$T^* = kT/\epsilon$

$\epsilon$  = depth of the potential well

$\sigma$  = distance at which the interaction energy is zero

$f_D^{(m)}$  = contribution of the Sonine expansion up to  $m^{\text{th}}$  order

$x$  = molar concentration of the lighter component  
 12 = subscript indicating a mixture of species 1 and 2.

In the first approximation,  $[D_{12}]_1$ , only the mixed interaction appears, but the higher approximations of  $D_{12}$  contain as well the interactions between like molecules. As  $f_D(x)$  differs slightly from unity the interactions between like molecules are always of minor importance. By comparing the experimental results with theory one can determine the potential parameters  $\epsilon_{12}$  and  $\sigma_{12}$ . However since  $\Omega^{(1,1)*}$  is a slowly varying function of temperature an accurate determination of the potential parameters is only possible from diffusion coefficients measured over a wide temperature range. Furthermore one needs measurements of  $D_{12}$  as a function of concentration in order to derive  $[D_{12}]_1$  from the experimental data.

We have performed diffusion measurements for a complete set of binary mixtures composed of the noble gases: He, Ne, Ar, Kr and Xe in the temperature range from 65°K to 400°K at pressures below 1 atm. The Chapman-Enskog theory in combination with a simple potential like the Lennard-Jones (12-6) potential is expected to be applicable to these gases. This has been tested both from the temperature and concentration dependence of  $D_{12}$ . For all mixtures the parameters  $\epsilon_{12}$  and  $\sigma_{12}$  have been derived. As the potential parameters of the pure noble gases are rather well known it is possible to investigate how the interactions between a pair of unlike molecules are related to interactions between like molecules.

2. *Experimental procedure.* For the determination of  $D_{12}$  we have used a two-chamber diffusion cell which is described in detail in chapter I. The procedure has been carefully checked for the system  $N_2$ - $H_2$ . We limit ourselves here to a schematic survey.

Two chambers, connected by a capillary, are initially filled with the same mixture. At time  $t = 0$  we set up a concentration difference,  $(\Delta x)_0$ , over the capillary by admitting some pure gas in one of the chambers. Then the diffusion coefficient is determined from the rate of change of  $\Delta x$ :

$$(\Delta x)_t = (\Delta x)_0 e^{-t/\tau} \quad (3)$$

where

$$\frac{1}{\tau} = D_{12} \frac{A}{l_{\text{cap}}} \left( \frac{1}{V^u} + \frac{1}{V^l} \right) (1 + \zeta). \quad (4)$$

In eq. (4)  $l_{\text{cap}}$  and  $A$  denote the capillary length and cross sectional area,  $V^u$  and  $V^l$  are the volumes of upper and lower chamber and  $\zeta$  is a correction arising from the volume as well as the end effects of the capillary.

The concentration difference is continuously registered using thermistors, placed into the apparatus.

Measurements have been performed at different temperatures with a

bath of liquid N<sub>2</sub>, O<sub>2</sub>, CH<sub>4</sub>, C<sub>2</sub>H<sub>4</sub> and C<sub>3</sub>H<sub>8</sub> boiling at constant pressure and with commercial thermostats, filled with water (295°K) or oil (400°K). The noble gases have the natural isotopic composition. The purity of the gases is at least 99.9%.

3. *Evaluation of the experimental data.* a. Determination of  $D_{12}$  at  $x = 0.5$  as a function of temperature. For conditions imposed by temperature stability and by the nature of the correction  $\zeta$  in eq. (4) this apparatus is only suitable to measure diffusion coefficients larger than  $10 \text{ cm}^2 \text{ s}^{-1}$ . Since in most cases  $D_{12}$  at 1 atm is much smaller than  $1 \text{ cm}^2 \text{ s}^{-1}$  we are forced to measure at rather low pressures (note  $D_{12} \sim 1/p$ ). At these low pressures, however, the mean free path,  $\ell$ , is not very small as compared to the radius of the capillary,  $r_{\text{cap}}$ . Therefore the diffusion coefficient as calculated from the eqs. (3) and (4) has to be corrected for the occurrence of "Knudsen" effects. When  $\ell/r_{\text{cap}}$  is not too large one can describe the "Knudsen" effect with an expression of the form:

$$(D_{12}p)_{\text{Kn}}^{\text{exp}} = D_{12}p \left( 1 - c_1 \frac{\ell}{r_{\text{cap}}} \right). \quad (5)$$

Here  $(D_{12}p)_{\text{Kn}}^{\text{exp}}$  refers to the apparent diffusion coefficient as calculated from the measured value of  $\tau$  (see eq. (4)).  $c_1$  is a coefficient of the order unity; its value might depend on the nature of the capillary surface and accommodation coefficient. We can determine its value experimentally. We therefore rewrite eq. (5), using  $\ell \sim T/p$ , as:

$$(D_{12}p)_{\text{Kn}}^{\text{exp}} = D_{12}p \left( 1 - c_2 \frac{T}{pr_{\text{cap}}} \right) \quad (6)$$

where  $c_2$  denotes a constant which includes  $c_1$ .

For a mixture at  $x = 0.5$  we plot  $(D_{12}p)_{\text{Kn}}^{\text{exp}}$  as a function of  $1/pr_{\text{cap}}$  at constant temperature (see *e.g.* fig. 1 of section 4; for simplicity we only use one symbol to denote the averaged value obtained from four diffusion runs). The experiments show that eq. (6) holds for a reasonable value of  $c_2$ . The true value of  $(D_{12}p)^{\text{exp}}$  is determined by extrapolating  $1/pr_{\text{cap}}$  to zero.

A further check on relation (6) is obtained from the slopes of the lines in fig. 1 in the following way. From eq. (6) we derive:

$$-\frac{1}{D_{12}p} \frac{d(D_{12}p)_{\text{Kn}}^{\text{exp}}}{d(1/pr_{\text{cap}})} = -c_2 T. \quad (7)$$

We plot the left hand side of eq. (7) vs. temperature (see *e.g.* fig. 2 of section 4). In general eq. (7) is well satisfied. This gives a further justification of the procedure used.

b. Determination of  $D_{12}$  as a function of concentration. Since for the determination of  $D_{12}$  at a fixed concentration a large number of measurements are needed to obtain an accuracy of say 0.5% in the extrapolation procedure, we do not follow the method of section 3a for the other concentrations. In a number of checks the constant  $c_2$  in eq. (6) appeared to be concentration independent. We can therefore use the values of  $c_2$  obtained at  $x = 0.5$  to correct  $(D_{12}p)_{\text{Kn}}^{\text{exp}}$  at all concentrations. Hence we measure  $(D_{12}p)_{\text{Kn}}^{\text{exp}}$  as a function of concentration at a fixed pressure and apply the Knudsen correction as calculated from eq. (6), using for  $c_2$  the value as determined at  $x = 0.5$ .

In our method it is only possible to measure diffusion coefficients in the concentration range, extending from  $x = 0.10$  to  $x = 0.90$ . Due to lack of accuracy in the individual diffusion runs (1–2%) the extrapolation of  $D_{12}$  to the ends of the concentration range, without the help of theory, is rather questionable. Therefore we consider the concentration dependent part of eq. (1):  $f_D(x)$ . We restrict ourselves to the second approximation<sup>4</sup>):

$$f_D^{(2)} = 1 + \frac{(6C_{12}^* - 5)^2}{10} A(x) \quad (8)$$

In this expression  $C_{12}^*$  (ratio of  $\Omega_{12}^{(1,2)*}$  to  $\Omega_{12}^{(1,1)*}$ ) is strongly dependent on the intermolecular potential, but not on  $x$ , whereas the function  $A(x)$  is almost completely determined by the molecular weights and concentrations of the constituents of the mixture. In order to eliminate the influence of the potential model only the dependence of  $A$  on  $x$  is used in the extrapolation of  $D_{12}$  to  $x = 0$  and  $x = 1$ . If we write  $f_D^{(2)} = 1 + FA(x)$ , the shape of the curve  $f_D^{(2)}$  is fixed through  $A(x)$  whereas  $F$  may be considered as a scale factor following from the experimental data. We proceed in the following way. We plot the experimental values of  $(D)_x/(D)_{x=0.5}$  as a function of  $x$  and make a best fit with  $(1 + FA_x)/(1 + FA_{x=0.5})$  through an adjustment of  $F$  by trial and error (see e.g. fig. 3 in section 4; to avoid double subscripts of  $D_{12}$  we omit in this case the subscript 12). Now  $F$  can be compared with the term  $(6C_{12}^* - 5)^2/10$ , where the potential model appears. This is done in e.g. fig. 4 of section 4 by plotting  $(D)_{x=1}/(D)_{x=0}$  vs. temperature and the curve of  $f_{x=1}^{(2)}/f_{x=0}^{(2)}$  as calculated for the L.J. (12-6) potential (second Kihara approximation<sup>4</sup>)<sup>5</sup>). A further discussion is given in section 7.

c. Determination of the potential parameters. In order to find  $\epsilon_{12}$  and  $\sigma_{12}$  we fit the measurements to the Chapman-Enskog expression  $[D_{12}]_1$  (see eq. (2)) in the following way. From  $(D_{12}p)_{x=0.5}^{\text{exp}}$  we calculate  $(D_{12}p)_{x=1}^{\text{exp}}$  by using the concentration dependence as determined in section 3b. The advantage of this choice is that at this concentration  $f_D$  differs no more than  $10^{-4}$  from unity, hence one can identify  $(D_{12})_{x=1}^{\text{exp}}$  with  $[D_{12}]_1$ . We now write eq. (2) with reduced quantities (see chapter I, eqs. (14)

and (15)):

$$\frac{[D_{12}]_1^* \rho_{12}^*}{\sqrt{T_{12}^{*3}}} = \frac{[D_{12}]_1 \phi}{\sqrt{k^3 T^3 / 2\mu_{12}}} \sigma_{12}^2 = \frac{3/8 \sqrt{\pi}}{\Omega_{12}^{(1,1)*}(T_{12}^*)}. \quad (9)$$

By curve shifting we make coincide  $\log\{(D_{12})_{x=1}^{\text{exp}} \phi / \sqrt{k^3 T^3 / 2\mu_{12}}\}$  vs.  $\log T$  and  $\log\{[D_{12}]_1^* \rho_{12}^* / \sqrt{T_{12}^{*3}}\}$  vs.  $\log T_{12}^*$ . In this way one obtains  $(\epsilon/k)_{12}$  and  $\sigma_{12}^2$ . A typical plot as used is shown in fig. 5 for the system Ne-He (L.J. (12-6) potential). As one can see from the slight curvature it is hardly possible to derive independently  $(\epsilon/k)_{12}$  and  $\sigma_{12}$ . This is illustrated by the dashed line drawn for a 5°K lower value of  $(\epsilon/k)_{12}$ . The accuracy in  $\epsilon/k$  is worse than in  $\sigma$  (see scales of fig. 5). The best fit with a straight line for  $\log\{(D_{12})_{x=1}^{\text{exp}} \phi / \sqrt{k^3 T^3 / 2\mu_{12}}\}$  vs.  $\log T$  determines, however, rather accurately the quantity  $(\epsilon/k)_{12} \sigma_{12}^n$ . Here  $n$  depends on the slope of the line. Without much loss in accuracy only integral values of  $n$  can be used, giving  $n = 11$  in the case of Ne-He. An accurate value of  $(\epsilon/k)_{12} \sigma_{12}^n$  is still useful for the comparison with other mixtures in order to test the combination rules. This will be described in section 7.

We have investigated the L.J. (12-6) potential and the (exp-6) potential with for  $\alpha$  the values: 12, 13, 14 and 15. For the L.J. potential we use the parameters  $\epsilon$  and  $\sigma$ ; the (exp-6) potential takes its simplest form, however, with  $\epsilon$  and  $r_m$  (distance for minimum energy), so we shall report either  $\sigma$  or  $r_m$  corresponding to the potential under consideration. In general all potential models fit the experiments for a suitable choice of  $\epsilon$  and  $\sigma$ . For every model the best set of  $\epsilon$  and  $\sigma$  is determined. Finally we conclude to the best potential model from the standard deviation of the experimental data with respect to the theoretical curve with the optimal values for  $\epsilon$  and  $\sigma$  in e.g. fig. 5.

The procedure is performed using  $\Omega^{(1,1)*}$ -data from refs. 6 and 7. Quantum mechanical corrections, especially important for mixtures with He, are applied in the same way as in the case of N<sub>2</sub>-H<sub>2</sub> (see chapter I).

4. *Results.* In this section we shall report the results for all binary mixtures of the noble gases, obtained in the way as described in section 3. We shall limit the discussion to remarks that are pertinent only to the system under consideration. We shall present a comparison with the results of other sources in the next section (5), while a general discussion of the potential parameters obtained is postponed to sections 6 and 7. In section 7 also the concentration dependence of  $D_{12}$  is discussed in general.

Systems:

a. Ne-He. For this mixture  $D_{12}$  at  $x = 0.5$  has been measured between 65°K and 295°K. The lower temperature limit is determined by the availability of a stable cooling liquid. Liquefied neon has not been used since at this temperature the diffusion coefficient is too small to measure accurately with

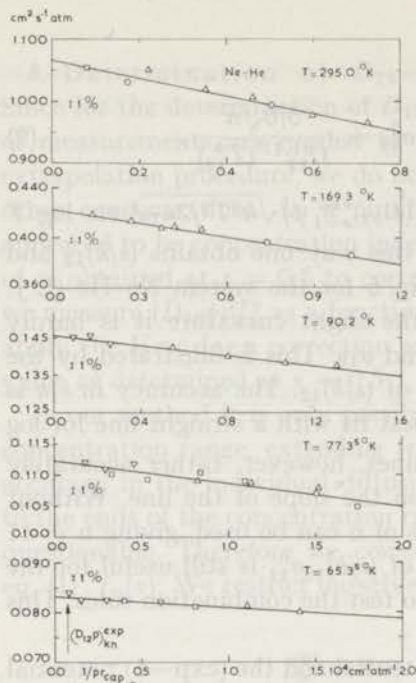


Fig. 1. Mean free path dependence of the diffusion coefficient at different temperatures;  $x = 0.5$ .

- $\nabla$   $r_{\text{cap}} = 0.1372$  cm
- $\square$   $r_{\text{cap}} = 0.1008$  cm
- $\triangle$   $r_{\text{cap}} = 0.0699$  cm
- $\circ$   $r_{\text{cap}} = 0.0453$  cm

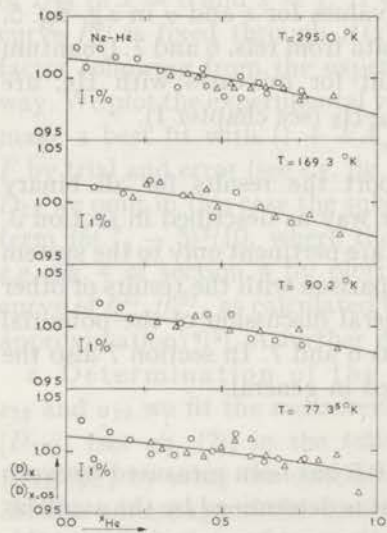


Fig. 3. Concentration dependence of the diffusion coefficient at different temperatures.

- $\circ$  He-diffusion run
- $\triangle$  Ne-diffusion run

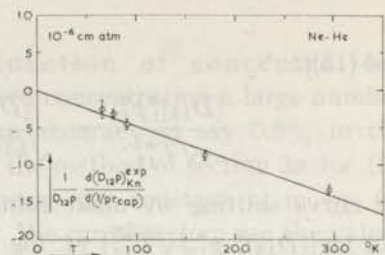


Fig. 2. Mean free path dependence of the diffusion coefficient as a function of temperature;  $x = 0.5$ .

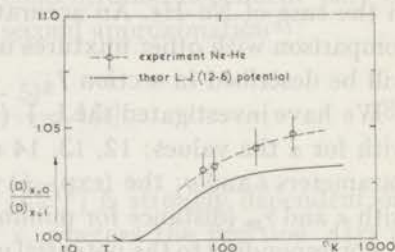


Fig. 4. Concentration dependence of the diffusion coefficient as a function of temperature.

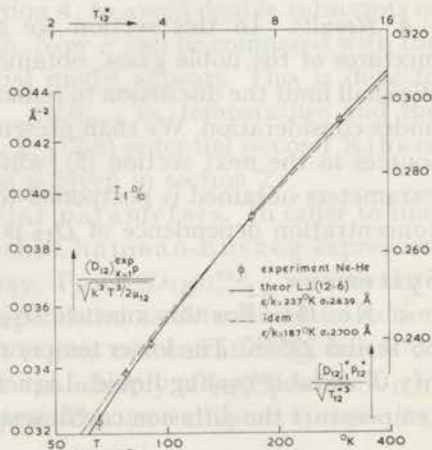


Fig. 5. Determination of the potential parameters for the system Ne-He.



this method. As the determination of the concentration dependence needs a still better temperature stability (see section 3b), no measurements are done at 65°K (reduced liquid nitrogen bath).

The results for  $(D_{12}p)_{x=0.5}$  as a function of  $1/p r_{\text{cap}}$  are collected in fig. 1. The influence of the "Knudsen" effect as a function of temperature is shown in fig. 2. In fig. 3 the concentration dependence is plotted at various temperatures and in fig. 4 one sees the results as a function of temperature, together with the curve for the Lennard-Jones (12-6) potential. Although the concentration dependence has the same form as predicted from theory, no agreement is found for the absolute value (see section 7).

In table I, second column, we have collected the extrapolated values of  $(D_{12}p)_{x=0.5}^{\text{exp}}$  from fig. 1. In the third column we have given the ratio of  $(D)_{x=0.5}$  to  $(D)_{x=1.0}$  as calculated from the smoothed experimental curve in fig. 4. In the last column the slopes of the lines in fig. 1 are reported ("Knudsen" effect).

The results for the potential parameters are collected in table II. For this mixture we do not use the (exp-6) potential,  $\alpha = 12$  and  $\alpha = 13$ , because these models cannot be fitted to the experimental data. Results are only reported with  $\alpha = 14$  and  $\alpha = 15$ .

From the standard deviation given in the second column of table II the Lennard-Jones potential is concluded to be the best fitting model (see also fig. 5). In the last two columns of this table we give the results for  $(\epsilon/k)_{12} (r_m)_{12}^{11}$  and  $(\epsilon/k)_{12} \sigma_{12}^{11}$ , resp., as calculated from the straight line fitting procedure.

TABLE I

| Experimental results for the system Ne-He |  |                                   |  |
|---|--|-----------------------------------|--|
| Temperature<br>°K                         | $D_{12}p$ for $x = 0.5$<br>$10^{-2} \text{ cm}^2 \text{ s}^{-1} \text{ atm}$ | $\frac{(D)_{x=0.5}}{(D)_{x=1.0}}$ | $\frac{1}{D_{12}p} \frac{d(D_{12}p)_{\text{Kn}}^{\text{exp}}}{d(1/pr_{\text{cap}})}$<br>$10^{-6} \text{ cm atm}$ |
| 65.3 <sup>s</sup>                         | $8.34 \pm 0.08$  | $1.018 \pm 0.004$                 | $-(2.5 \pm 1.1)$   |
| 77.3 <sup>s</sup>                         | $11.25 \pm 0.05$   | $1.019 \pm 0.004$                 | $-(3.2 \pm 0.6)$   |
| 90.2                                      | $14.58 \pm 0.08$   | $1.021 \pm 0.004$                 | $-(4.6 \pm 0.6)$   |
| 169.3                                     | $42.4 \pm 0.2$   | $1.027 \pm 0.005$                 | $-(8.7 \pm 0.6)$   |
| 295.0                                     | $106.8 \pm 0.6$  | $1.030 \pm 0.005$                 | $-(13.4 \pm 0.6)$  |

TABLE II

| Potential parameters for the system Ne-He, derived from the diffusion coefficient |                         |                           |                   |                    |  |   |
|---|-------------------------|---------------------------|-------------------|--------------------|--|---|
| Potential   | Standard deviation<br>% | $(\epsilon/k)_{12}$<br>°K | $(r_m)_{12}$<br>Å | $\sigma_{12}$<br>Å | $(\epsilon/k)_{12} (r_m)_{12}^{11}$<br>$10^6 \text{ } ^\circ\text{K } \text{Å}^{11}$ | $(\epsilon/k)_{12} \sigma_{12}^{11}$<br>$10^6 \text{ } ^\circ\text{K } \text{Å}^{11}$ |
| Exp - 6, $\alpha = 14$  | 0.7                     | $12.6 \pm 4.0$            | $3.20 \pm 0.09$   |                    | $4.53 \pm 0.03$  |   |
| „ $\alpha = 15$   | 0.4                     | $20.5 \pm 2.0$            | $3.01 \pm 0.03$   |                    | $3.73 \pm 0.02$  |   |
| Lennard-Jones<br>(12-6)   | 0.3                     | $23.7 \pm 2.0$            |                   | $2.64 \pm 0.02$    |  | $1.03 \pm 0.01$   |

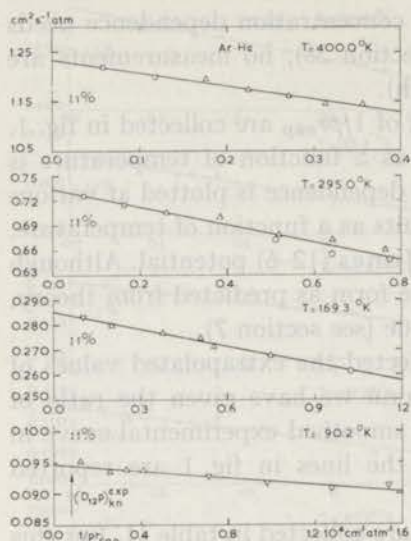


Fig. 6. Mean free path dependence of the diffusion coefficient at different temperatures;  $x = 0.5$ .

- ▽  $r_{\text{cap}} = 0.1372$  cm
- $r_{\text{cap}} = 0.1008$  cm
- △  $r_{\text{cap}} = 0.0699$  cm
- $r_{\text{cap}} = 0.0453$  cm

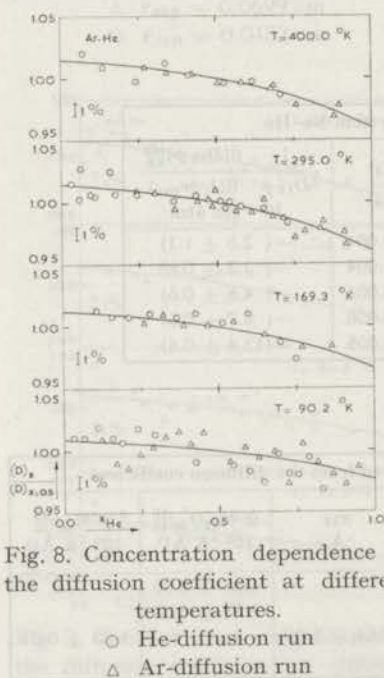


Fig. 8. Concentration dependence of the diffusion coefficient at different temperatures.

- He-diffusion run
- △ Ar-diffusion run

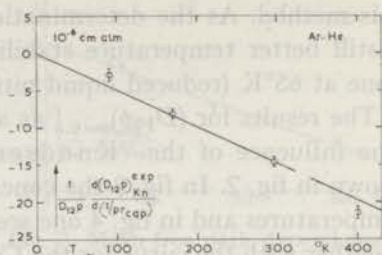


Fig. 7. Mean free path dependence of the diffusion coefficient as a function of temperature;  $x = 0.5$ .

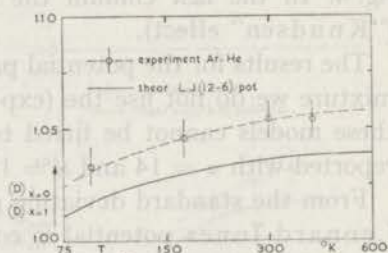


Fig. 9. Concentration dependence of the diffusion coefficient as a function of temperature.

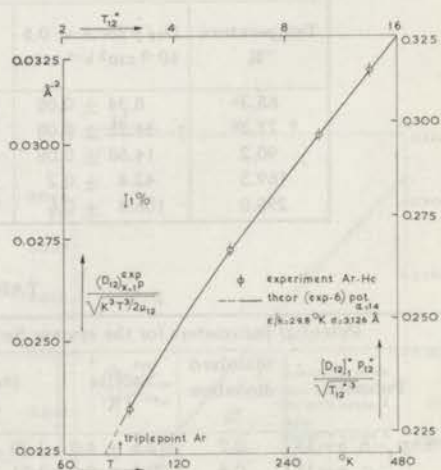


Fig. 10. Determination of the potential parameters for the system Ar-He.

Although the quantum mechanical influence on the diffusion coefficient is no more than 3% the effect on  $\epsilon/k$  and  $\sigma$  is large:  $\epsilon/k$  as obtained classically turns out to be 7°K lower and  $\sigma$  is increased with about 0.07Å; the value of  $(\epsilon/k)_{12}\sigma_{12}^{11}$ , however, is rather insensitive to this correction and does not change more than a few percent.

b. Ar-He. This mixture has been measured at different concentrations in the temperature range between 90°K and 400°K. The lower temperature is limited by the triple point of argon. The results are presented in the same form as in the preceding part of this section. Table III is obtained from the figs. 6, 7, 8 and 9. Again no agreement with theory is obtained for the concentration dependence of  $D_{12}$  as a function of temperature (see fig. 9). The values obtained for the potential parameters are given in table IV (see fig. 10).

The influence of the quantum mechanical corrections is approximately 4°K in  $(\epsilon/k)_{12}$  and 0.03 Å in  $\sigma_{12}$ .

TABLE III

| Experimental results for the system Ar-He |   |                                   |   |
|---|---|-----------------------------------|---|
| Temperature<br>°K                         | $D_{12} p$ for $x = 0.5$<br>$10^{-2} \text{ cm}^2 \text{ s}^{-1} \text{ atm}$ | $\frac{(D)_{x=0.5}}{(D)_{x=1.0}}$ | $\frac{1}{D_{12} p} \frac{d(D_{12} p)_{\text{Kn}}^{\text{exp}}}{d(1/p r_{\text{exp}})}$<br>$10^{-6} \text{ cm atm}$ |
| 90.2                                      | $9.48 \pm 0.08$   | $1.023 \pm 0.004$                 | $-(2.9 \pm 0.9)$  |
| 169.3                                     | $28.53 \pm 0.15$  | $1.033 \pm 0.005$                 | $-(8.1 \pm 0.6)$  |
| 295.0                                     | $73.4 \pm 0.4$  | $1.039 \pm 0.006$                 | $-(14.6 \pm 0.6)$   |
| 400.0                                     | $123.3 \pm 0.6$   | $1.041 \pm 0.006$                 | $-(21.4 \pm 0.7)$   |

TABLE IV

| Potential parameters for the system Ar-He, derived from the diffusion coefficient |                         |                           |                   |                    |  |   |
|---|-------------------------|---------------------------|-------------------|--------------------|--|---|
| Potential   | Standard deviation<br>% | $(\epsilon/k)_{12}$<br>°K | $(r_m)_{12}$<br>Å | $\sigma_{12}$<br>Å | $(\epsilon/k)_{12}(r_m)_{12}^{10}$<br>$10^6 \text{ °K Å}^{10}$ | $(\epsilon/k)_{12}\sigma_{12}^{10}$<br>$10^6 \text{ °K Å}^{10}$ |
| Exp -6, $\alpha = 13$   | 0.6                     | $21.0 \pm 3.5$            | $3.72 \pm 0.06$   |                    | $10.45 \pm 0.08$   |   |
| „ $\alpha = 14$   | 0.1                     | $29.8 \pm 4.0$            | $3.51 \pm 0.05$   |                    | $8.54 \pm 0.06$  |   |
| „ $\alpha = 15$   | 0.3                     | $35.7 \pm 3.0$            | $3.40 \pm 0.03$   |                    | $7.29 \pm 0.05$  |   |
| Lennard-Jones<br>(12-6)   | 0.4                     | $40.2 \pm 3.0$            |                   | $2.98 \pm 0.02$    |  | $2.23 \pm 0.02$   |

c. Kr-He. This mixture is studied at  $x = 0.5$  from 112°K to 400°K. The lower temperature is limited by the triple point of Kr. The concentration dependence is measured from 169°K to 400°K. The results are presented in the figs. 11-15 and the tables V and VI. For the influence of the concentration on  $D_{12}$  fig. 14 shows the same tendency as obtained in the earlier parts of this section. The results for the potential parameters are

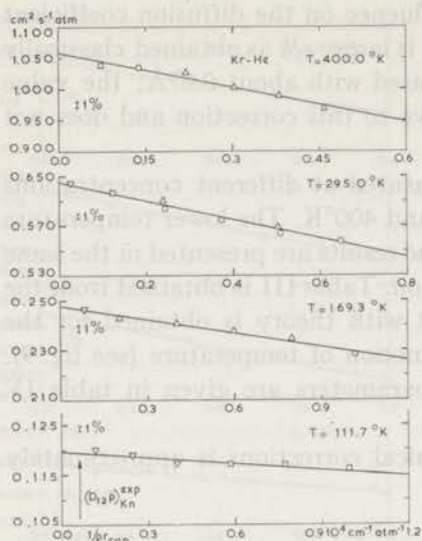


Fig. 11. Mean free path dependence of the diffusion coefficient at different temperatures;  $x = 0.5$ .

- ▽  $r_{cap} = 0.1372$  cm
- $r_{cap} = 0.1008$  cm
- △  $r_{cap} = 0.0699$  cm
- $r_{cap} = 0.0453$  cm

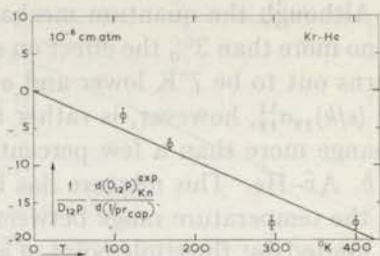


Fig. 12. Mean free path dependence of the diffusion coefficient as a function of temperature;  $x = 0.5$ .

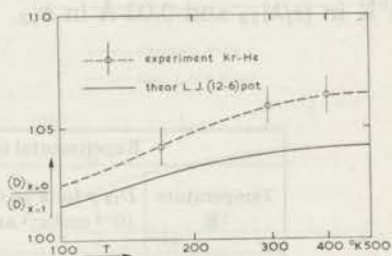


Fig. 14. Concentration dependence of the diffusion coefficient as a function of temperature.

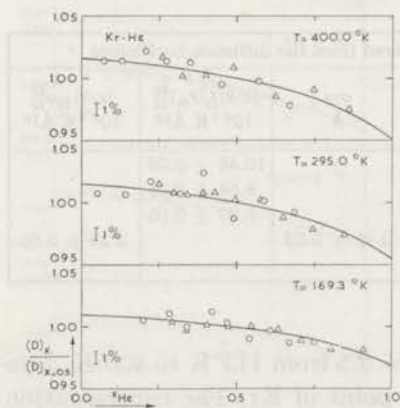


Fig. 13. Concentration dependence of the diffusion coefficient at different temperatures.

- He-diffusion run
- △ Kr-diffusion run

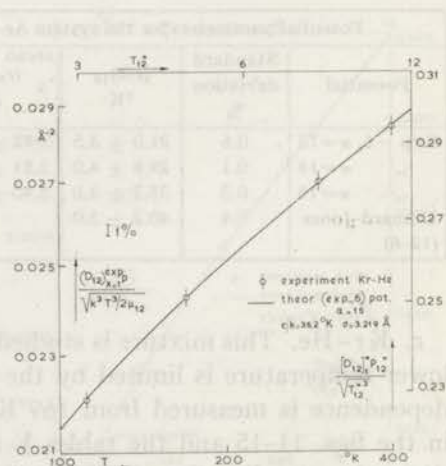


Fig. 15. Determination of the potential parameters for the system Kr-He.

less accurate than for the earlier mentioned systems since the curvature of  $\log\{(D_{12})_{x=1}^{\text{exp}}/p/\sqrt{k^3T^3/2\mu_{12}}\}$  vs.  $\log T$  is somewhat less (see fig. 15 and table VI). Quantum mechanical calculations correct the obtained parameters by about  $4^\circ\text{K}$  in  $(\epsilon/k)_{12}$  and  $0.03 \text{ \AA}$  in  $\sigma_{12}$ .

TABLE V

| Experimental results for the system Kr-He |   |                                   |  |
|---|---|-----------------------------------|--|
| Temperature<br>°K                         | $D_{12} p$ for $x = 0.5$<br>$10^{-2} \text{ cm}^2 \text{ s}^{-1} \text{ atm}$ | $\frac{(D)_{x=0.5}}{(D)_{x=1.0}}$ | $\frac{1}{D_{12} p} \frac{d(D_{12} p)_{\text{Kn}}^{\text{exp}}}{d(1/pr_{\text{exp}})}$<br>$10^{-6} \text{ cm atm}$ |
| 111.7                                     | $11.97 \pm 0.10$  | $1.021 \pm 0.004$                 | $-(3.3 \pm 1.0)$   |
| 169.3                                     | $24.79 \pm 0.15$  | $1.031 \pm 0.005$                 | $-(7.3 \pm 0.6)$   |
| 295.0                                     | $64.3 \pm 0.4$  | $1.044 \pm 0.006$                 | $-(17.7 \pm 0.8)$  |
| 400.0                                     | $105.9 \pm 0.6$   | $1.048 \pm 0.007$                 | $-(17.7 \pm 0.8)$  |

TABLE VI

| Potential parameters for the system Kr-He, derived from the diffusion coefficient |                         |                           |                   |                    |  |   |
|---|-------------------------|---------------------------|-------------------|--------------------|--|---|
| Potential   | Standard deviation<br>% | $(\epsilon/k)_{12}$<br>°K | $(r_m)_{12}$<br>Å | $\sigma_{12}$<br>Å | $(\epsilon/k)_{12}(r_m)_{12}^{10}$<br>$10^7 \text{ }^\circ\text{K} \text{ \AA}^{10}$ | $(\epsilon/k)_{12}\sigma_{12}^{10}$<br>$10^6 \text{ }^\circ\text{K} \text{ \AA}^{10}$ |
| Exp -6, $\alpha=13$   | 0.9                     | $23.6 \pm 6.0$            | $3.89 \pm 0.10$   |                    | $1.85 \pm 0.02$  |   |
| „ $\alpha=14$   | 0.3                     | $28.5 \pm 5.0$            | $3.74 \pm 0.07$   |                    | $1.53 \pm 0.02$  |   |
| „ $\alpha=15$   | 0.1                     | $36.2 \pm 6.0$            | $3.60 \pm 0.06$   |                    | $1.31 \pm 0.01$  |   |
| Lennard-Jones<br>(12-6)   | 0.2                     | $39.0 \pm 5.0$            |                   | $3.17 \pm 0.04$    |  | $4.05 \pm 0.03$   |

TABLE VII

| Experimental results for the system Xe-He |   |                                   |  |
|---|---|-----------------------------------|--|
| Temperature<br>°K                         | $D_{12} p$ for $x = 0.5$<br>$10^{-2} \text{ cm}^2 \text{ s}^{-1} \text{ atm}$ | $\frac{(D)_{x=0.5}}{(D)_{x=1.0}}$ | $\frac{1}{D_{12} p} \frac{d(D_{12} p)_{\text{Kn}}^{\text{exp}}}{d(1/pr_{\text{exp}})}$<br>$10^{-6} \text{ cm atm}$ |
| 169.3                                     | $21.34 \pm 0.15$  | $1.036 \pm 0.006$                 | $-(8.5 \pm 0.8)$   |
| 231.1                                     | $35.7 \pm 0.2$  | $1.045 \pm 0.007$                 | $-(9.9 \pm 0.6)$   |
| 295.0                                     | $54.9 \pm 0.3$  | $1.049 \pm 0.007$                 | $-(12.6 \pm 0.6)$  |
| 400.0                                     | $91.8 \pm 0.6$  | $1.053 \pm 0.008$                 | $-(17.9 \pm 0.7)$  |

TABLE VIII

| Potential parameters for the system Xe-He, derived from the diffusion coefficient |                         |                           |                   |                    |  |   |
|---|-------------------------|---------------------------|-------------------|--------------------|--|---|
| Potential   | Standard deviation<br>% | $(\epsilon/k)_{12}$<br>°K | $(r_m)_{12}$<br>Å | $\sigma_{12}$<br>Å | $(\epsilon/k)_{12}(r_m)_{12}^{10}$<br>$10^7 \text{ }^\circ\text{K} \text{ \AA}^{10}$ | $(\epsilon/k)_{12}\sigma_{12}^{10}$<br>$10^6 \text{ }^\circ\text{K} \text{ \AA}^{10}$ |
| Exp -6, $\alpha=14$   | 1.2                     | $41.9 \pm 6.0$            | $3.88 \pm 0.05$   |                    | $3.27 \pm 0.03$  |   |
| „ $\alpha=15$   | 1.0                     | $43.0 \pm 7.0$            | $3.82 \pm 0.06$   |                    | $2.85 \pm 0.02$  |   |
| Lennard-Jones<br>(12-6)   | 1.1                     | $46.5 \pm 7.0$            |                   | $3.37 \pm 0.05$    |  | $8.83 \pm 0.06$   |

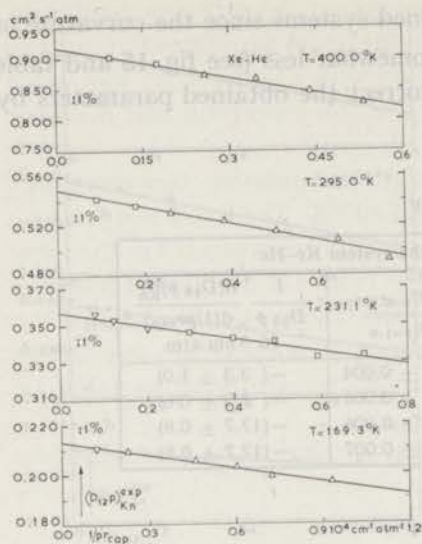


Fig. 16. Mean free path dependence of the diffusion coefficient at different temperatures;  $x = 0.5$ .

- $\nabla$   $r_{\text{cap}} = 0.1372$  cm
- $\square$   $r_{\text{cap}} = 0.1008$  cm
- $\triangle$   $r_{\text{cap}} = 0.0699$  cm

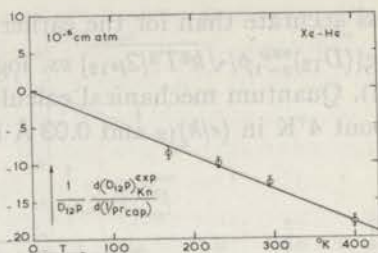


Fig. 17. Mean free path dependence of the diffusion coefficient as a function of temperature;  $x = 0.5$ .

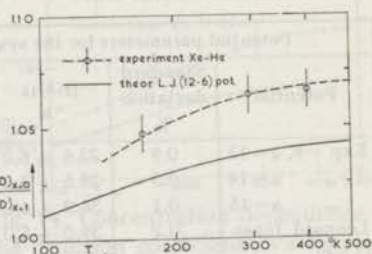


Fig. 19. Concentration dependence of the diffusion coefficient as a function of temperature.

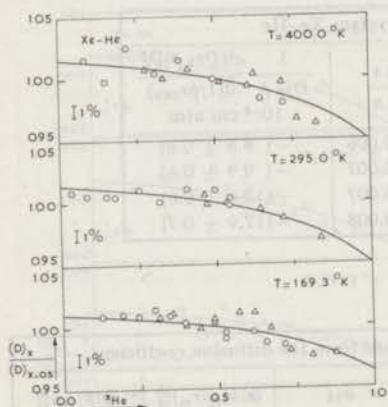


Fig. 18. Concentration dependence of the diffusion coefficient at different temperatures.

- $\circ$  He-diffusion run
- $\triangle$  Xe-diffusion run

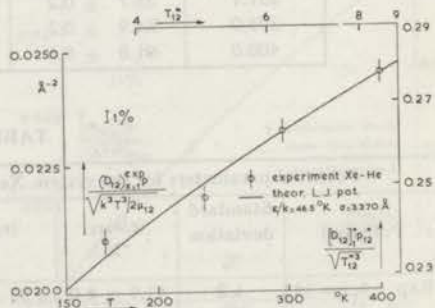


Fig. 20. Determination of the potential parameters for the system Xe-He.

d. Xe-He.  $D_{12}$  at all concentrations has been measured from 169°K to 400°K. The triple point of Xe makes the remaining temperature range very unfavourable for the determination of potential parameters but this mixture can still be used to obtain an accurate value of  $(\epsilon/k)_{12}\sigma_{12}^n$ . The results are collected in the figs. 16-20 and the tables VII and VIII. Again no agreement is obtained for the concentration dependence of  $D_{12}$  as a function of temperature (see fig. 19).

Even at the rather high temperatures as used for the mixture Xe-He quantum mechanical influences are still important: 4°K in  $(\epsilon/k)_{12}$  and 0.03 Å in  $\sigma_{12}$ .

e. Ar-Ne.  $D_{12}$  at  $x = 0.5$  has been measured from 90°K to 400°K. The temperature interval corresponds to the range of  $T^*$  from 1.5 to 7. As the largest curvature of the  $\Omega^{(1,1)}$ -function is appearing between  $T^* = 1$  and  $T^* = 5$  the mixture Ar-Ne is very suitable to determine uniquely the potential parameters.

The concentration dependence of  $D_{12}$  is small, so we only have measured it from 90°K to 295°K. The agreement with theory is good. The results are given in the figs. 21-25 and the tables IX and X.

The non-classical behaviour is of minor importance here: 1°K in  $(\epsilon/k)_{12}$  and 0.01 Å in  $\sigma_{12}$ . For the now following mixtures no quantum mechanical corrections have to be applied anymore.

TABLE IX

| Experimental results for the system Ar-Ne |   |                                   |  |
|---|---|-----------------------------------|--|
| Temperature<br>°K                         | $D_{12} p$ for $x = 0.5$<br>$10^{-2} \text{ cm}^2 \text{ s}^{-1} \text{ atm}$ | $\frac{(D)_{x=0.5}}{(D)_{x=1.0}}$ | $\frac{1}{D_{12} p} \frac{d(D_{12} p)_{\text{Kn}}^{\text{exp}}}{d(1/pr_{\text{exp}})}$<br>$10^{-6} \text{ cm atm}$ |
| 90.2                                      | $3.71 \pm 0.02$   | $1.002 \pm 0.001$                 | $-(2.5 \pm 0.8)$   |
| 169.3                                     | $12.02 \pm 0.07$  | $1.005 \pm 0.002$                 | $-(5.9 \pm 0.6)$   |
| 295.0                                     | $31.6 \pm 0.2$  | $1.009 \pm 0.003$                 | $-(9.7 \pm 0.6)$   |
| 400.0                                     | $53.0 \pm 0.3$  | $1.010 \pm 0.003$                 | $-(11.2 \pm 0.7)$  |

TABLE X

| Potential parameters for the system Ar-Ne, derived from the diffusion coefficient |                         |                           |                   |                    |  |   |
|---|-------------------------|---------------------------|-------------------|--------------------|--|---|
| Potential   | Standard deviation<br>% | $(\epsilon/k)_{12}$<br>°K | $(r_m)_{12}$<br>Å | $\sigma_{12}$<br>Å | $(\epsilon/k)_{12}(r_m)_{12}^7$<br>$10^5 \text{ °K Å}^7$ | $(\epsilon/k)_{12}\sigma_{12}^7$<br>$10^5 \text{ °K Å}^7$ |
| Exp -6, $\alpha=12$   | 1.1                     | $42.8 \pm 2.0$            | $3.83 \pm 0.03$   |                    | $5.15 \pm 0.04$  |   |
| „ $\alpha=13$   | 0.8                     | $49.8 \pm 2.0$            | $3.68 \pm 0.02$   |                    | $4.55 \pm 0.03$  |   |
| „ $\alpha=14$   | 0.7                     | $55.1 \pm 2.0$            | $3.58 \pm 0.02$   |                    | $4.17 \pm 0.03$  |   |
| „ $\alpha=15$   | 0.4                     | $60.9 \pm 2.0$            | $3.50 \pm 0.02$   |                    | $3.87 \pm 0.03$  |   |
| Lennard-Jones<br>(12-6)   | 0.3                     | $61.7 \pm 2.0$            |                   | $3.11 \pm 0.02$    |  | $1.71 \pm 0.01$   |

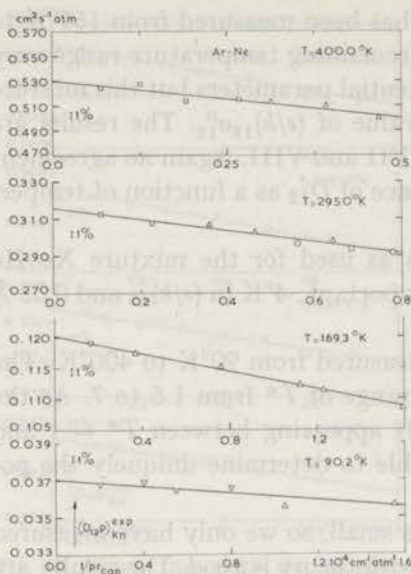


Fig. 21. Mean free path dependence of the diffusion coefficient at different temperatures;  $x = 0.5$ .

- ▽  $r_{cap} = 0.1372$  cm
- △  $r_{cap} = 0.1008$  cm
- $r_{cap} = 0.0699$  cm
- $r_{cap} = 0.0453$  cm

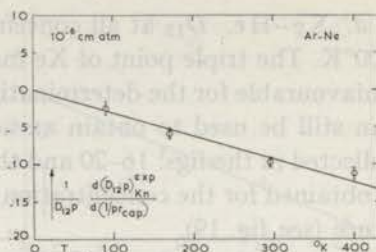


Fig. 22. Mean free path dependence of the diffusion coefficient as a function of temperature;  $x = 0.5$ .

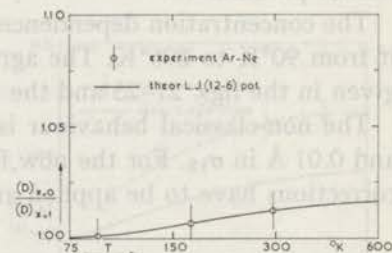


Fig. 24. Concentration dependence of the diffusion coefficient as a function of temperature.

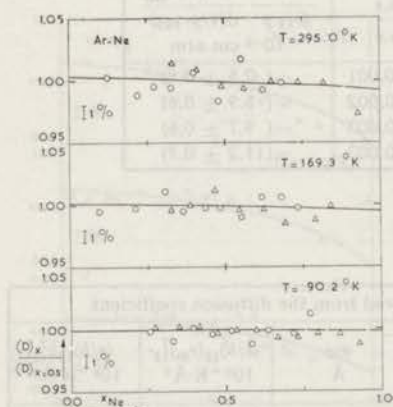


Fig. 23. Concentration dependence of the diffusion coefficient at different temperatures.

- Ne-diffusion run
- △ Ar-diffusion run

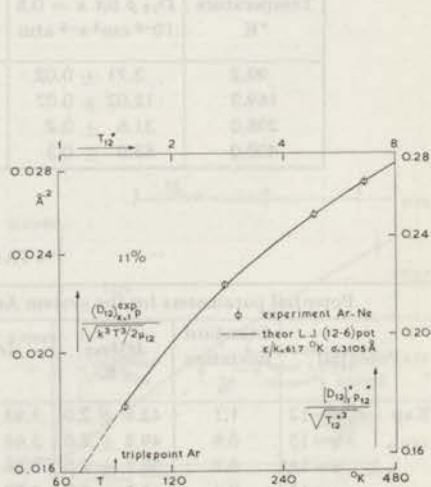


Fig. 25. Determination of the potential parameters for the system Ar-Ne.



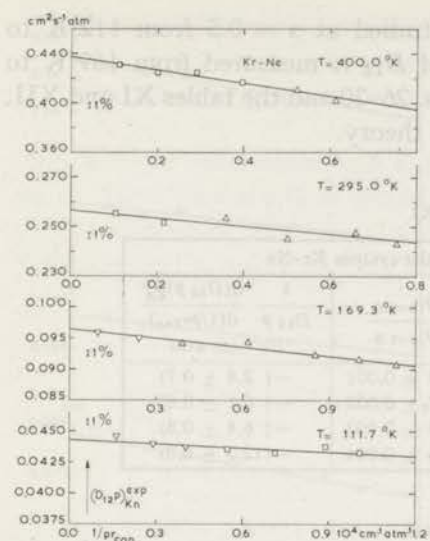


Fig. 26. Mean free path dependence of the diffusion coefficient at different temperatures;  $x = 0.5$ .

- $\nabla$   $r_{cap} = 0.1372$  cm
- $\square$   $r_{cap} = 0.1008$  cm
- $\triangle$   $r_{cap} = 0.0699$  cm

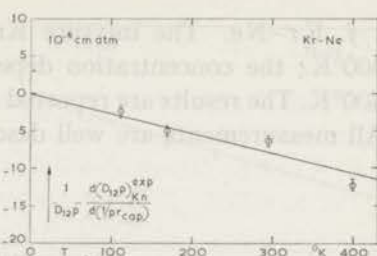


Fig. 27. Mean free path dependence of the diffusion coefficient as a function of temperature;  $x = 0.5$ .

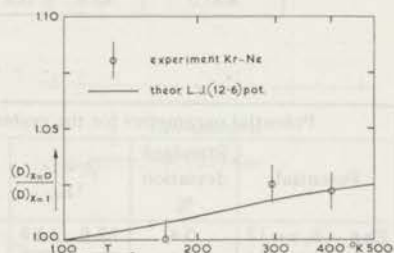


Fig. 29. Concentration dependence of the diffusion coefficient as a function of temperature.

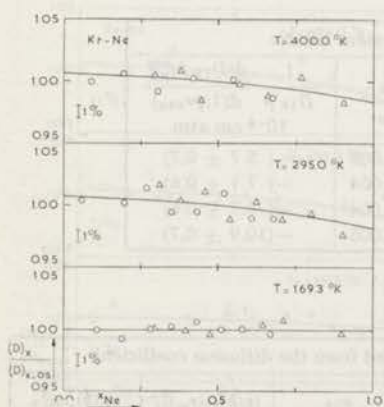


Fig. 28. Concentration dependence of the diffusion coefficient at different temperatures.

- $\circ$  Ne-diffusion run
- $\triangle$  Kr-diffusion run

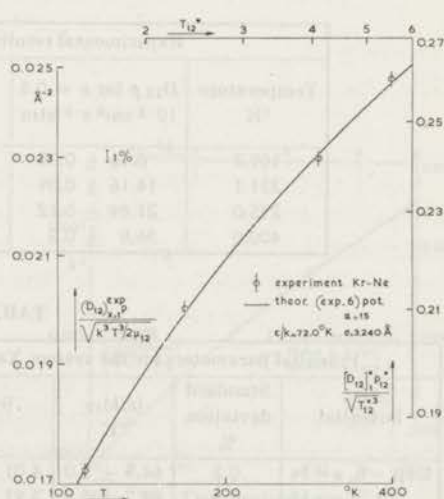


Fig. 30. Determination of the potential parameters for the system Kr-Ne.

f. Kr-Ne. The mixture Kr-Ne is studied at  $x = 0.5$  from 112°K to 400°K; the concentration dependence of  $D_{12}$  is measured from 169°K to 400°K. The results are reported in the figs. 26-30 and the tables XI and XII. All measurements are well described by theory.

TABLE XI

| Experimental results for the system Kr-Ne |   |                                   |   |
|---|---|-----------------------------------|---|
| Temperature<br>°K                         | $D_{12} p$ for $x = 0.5$<br>$10^{-2} \text{ cm}^2 \text{ s}^{-1} \text{ atm}$ | $\frac{(D)_{x=0.5}}{(D)_{x=1.0}}$ | $\frac{1}{D_{12} p} \frac{d(D_{12} p)_{\text{Kn}}^{\text{exp}}}{d(1/p r_{\text{exp}})}$<br>$10^{-6} \text{ cm atm}$ |
| 111.7                                     | $4.43 \pm 0.03$   | $1.003 \pm 0.001$                 | $-(2.4 \pm 0.7)$  |
| 169.3                                     | $9.65 \pm 0.05$   | $1.007 \pm 0.002$                 | $-(5.1 \pm 0.6)$  |
| 295.0                                     | $25.66 \pm 0.14$  | $1.013 \pm 0.003$                 | $-(6.4 \pm 0.8)$  |
| 400.0                                     | $43.8 \pm 0.3$  | $1.016 \pm 0.004$                 | $-(12.3 \pm 0.8)$   |

TABLE XII

| Potential parameters for the system Kr-Ne, derived from the diffusion coefficient |                         |                           |                   |                    |  |   |
|---|-------------------------|---------------------------|-------------------|--------------------|--|---|
| Potential   | Standard deviation<br>% | $(\epsilon/k)_{12}$<br>°K | $(r_m)_{12}$<br>Å | $\sigma_{12}$<br>Å | $(\epsilon/k)_{12}(r_m)_{12}^7$<br>$10^5 \text{ }^\circ\text{K } \text{Å}^7$ | $(\epsilon/k)_{12}\sigma_{12}^7$<br>$10^8 \text{ }^\circ\text{K } \text{Å}^7$ |
| Exp -6, $\alpha = 12$   | 0.4                     | $52.8 \pm 3.5$            | $3.94 \pm 0.04$   |                    | $7.76 \pm 0.06$  |   |
| „ $\alpha = 13$   | 0.4                     | $60.5 \pm 3.5$            | $3.80 \pm 0.03$   |                    | $6.94 \pm 0.05$  |   |
| „ $\alpha = 14$   | 0.4                     | $65.8 \pm 3.5$            | $3.71 \pm 0.03$   |                    | $6.35 \pm 0.05$  |   |
| „ $\alpha = 15$   | 0.3                     | $72.0 \pm 3.5$            | $3.62 \pm 0.03$   |                    | $5.91 \pm 0.05$  |   |
| Lennard-Jones<br>(12-6)   | 0.4                     | $69.8 \pm 3.5$            |                   | $3.24 \pm 0.02$    |  | $2.61 \pm 0.02$   |

TABLE XIII

| Experimental results for the system Xe-Ne |   |                                   |   |
|---|---|-----------------------------------|---|
| Temperature<br>°K                         | $D_{12} p$ for $x = 0.5$<br>$10^{-2} \text{ cm}^2 \text{ s}^{-1} \text{ atm}$ | $\frac{(D)_{x=0.5}}{(D)_{x=1.0}}$ | $\frac{1}{D_{12} p} \frac{d(D_{12} p)_{\text{Kn}}^{\text{exp}}}{d(1/p r_{\text{exp}})}$<br>$10^{-6} \text{ cm atm}$ |
| 169.3                                     | $8.16 \pm 0.05$   | $1.011 \pm 0.003$                 | $-(5.7 \pm 0.7)$  |
| 231.1                                     | $14.16 \pm 0.09$  | $1.017 \pm 0.004$                 | $-(7.1 \pm 0.6)$  |
| 295.0                                     | $21.84 \pm 0.12$  | $1.020 \pm 0.004$                 | $-(8.7 \pm 0.6)$  |
| 400.0                                     | $36.8 \pm 0.2$  | $1.024 \pm 0.005$                 | $-(10.9 \pm 0.7)$   |

TABLE XIV

| Potential parameters for the system Xe-Ne, derived from the diffusion coefficient |                         |                           |                   |                    |  |   |
|---|-------------------------|---------------------------|-------------------|--------------------|--|---|
| Potential   | Standard deviation<br>% | $(\epsilon/k)_{12}$<br>°K | $(r_m)_{12}$<br>Å | $\sigma_{12}$<br>Å | $(\epsilon/k)_{12}(r_m)_{12}^8$<br>$10^6 \text{ }^\circ\text{K } \text{Å}^8$ | $(\epsilon/k)_{12}\sigma_{12}^8$<br>$10^6 \text{ }^\circ\text{K } \text{Å}^8$ |
| Exp -6, $\alpha = 14$   | 0.2                     | $61.9 \pm 5.0$            | $4.01 \pm 0.04$   |                    | $4.09 \pm 0.03$  |   |
| „ $\alpha = 15$   | 0.2                     | $68.7 \pm 5.5$            | $3.91 \pm 0.04$   |                    | $3.75 \pm 0.03$  |   |
| Lennard-Jones<br>(12-6)   | 0.3                     | $69.1 \pm 6.0$            |                   | $3.48 \pm 0.04$    |  | $1.48 \pm 0.01$   |

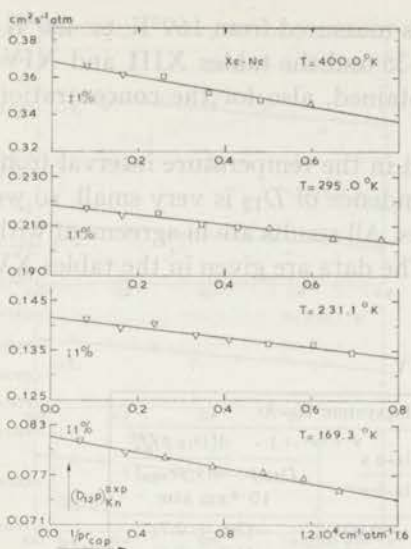


Fig. 31. Mean free path dependence of the diffusion coefficient at different temperatures;  $x = 0.5$ .

- $\nabla$   $r_{\text{cap}} = 0.1372$  cm
- $\square$   $r_{\text{cap}} = 0.1008$  cm
- $\triangle$   $r_{\text{cap}} = 0.0699$  cm

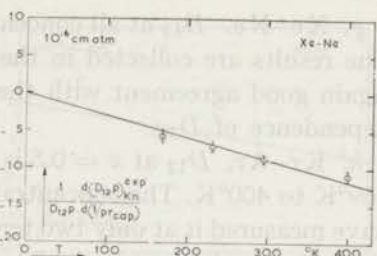


Fig. 32. Mean free path dependence of the diffusion coefficient as a function of temperature;  $x = 0.5$ .

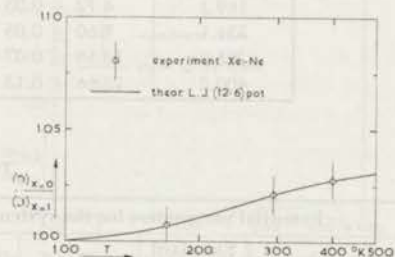


Fig. 34. Concentration dependence of the diffusion coefficient as a function of temperature.

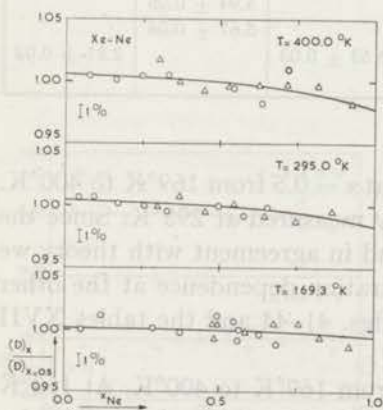


Fig. 33. Concentration dependence of the diffusion coefficient at different temperatures.

- $\circ$  Ne-diffusion run
- $\triangle$  Xe-diffusion run

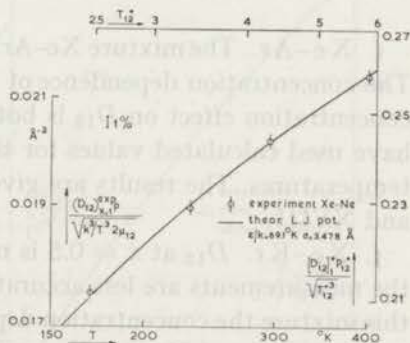


Fig. 35. Determination of the potential parameters for the system Xe-Ne.

g. Xe-Ne.  $D_{12}$  at all concentrations is measured from 169°K to 400°K. The results are collected in the figs. 31-35 and the tables XIII and XIV. Again good agreement with theory is obtained, also for the concentration dependence of  $D_{12}$ .

h. Kr-Ar.  $D_{12}$  at  $x = 0.5$  is measured in the temperature interval from 169°K to 400°K. The concentration dependence of  $D_{12}$  is very small, so we have measured it at only two temperatures. All results are in agreement with theory as can be seen in the figs. 36-40. The data are given in the tables XV and XVI.

TABLE XV

| Experimental results for the system Kr-Ar |   |                                   |  |
|---|---|-----------------------------------|--|
| Temperature<br>°K                         | $D_{12} p$ for $x = 0.5$<br>$10^{-2} \text{ cm}^2 \text{ s}^{-1} \text{ atm}$ | $\frac{(D)_{x=0.5}}{(D)_{x=1.0}}$ | $\frac{1}{D_{12} p} \frac{d(D_{12} p)_{\text{Kn}}^{\text{Exp}}}{d(1/pr_{\text{cap}})}$<br>$10^{-6} \text{ cm atm}$ |
| 169.3                                     | $4.72 \pm 0.03$   | $1.000 \pm 0.001$                 | $-(3.6 \pm 0.7)$   |
| 231.1                                     | $8.60 \pm 0.05$   | $1.001 \pm 0.001$                 | $-(4.7 \pm 0.6)$   |
| 295.0                                     | $13.58 \pm 0.07$  | $1.003 \pm 0.002$                 | $-(5.3 \pm 0.6)$   |
| 400.0                                     | $23.66 \pm 0.13$  | $1.005 \pm 0.002$                 | $-(6.8 \pm 0.6)$   |

TABLE XVI

| Potential parameters for the system Kr-Ar, derived from the diffusion coefficient |                            |                           |                   |                    |  |  |
|---|----------------------------|---------------------------|-------------------|--------------------|--|--|
| Potential   | Standard<br>deviation<br>% | $(\epsilon/k)_{12}$<br>°K | $(r_m)_{12}$<br>Å | $\sigma_{12}$<br>Å | $(\epsilon/k)_{12}(r_m)_{12}^6$<br>$10^5 \text{ °K Å}^6$ | $(\epsilon/k)_{12} \sigma_{12}^6$<br>$10^5 \text{ °K Å}^6$ |
| Exp -6, $\alpha=12$   | 0.3                        | $120 \pm 7$               | $4.22 \pm 0.04$   |                    | $6.80 \pm 0.05$  |  |
| " $\alpha=13$   | 0.1                        | $133 \pm 8$               | $4.10 \pm 0.04$   |                    | $6.29 \pm 0.05$  |  |
| " $\alpha=14$   | 0.1                        | $144 \pm 9$               | $4.01 \pm 0.04$   |                    | $5.94 \pm 0.05$  |  |
| " $\alpha=15$   | 0.1                        | $153 \pm 10$              | $3.93 \pm 0.04$   |                    | $5.67 \pm 0.04$  |  |
| Lennard-Jones<br>(12-6)   | 0.1                        | $145 \pm 8$               |                   | $3.53 \pm 0.03$    |  | $2.81 \pm 0.02$  |

i. Xe-Ar. The mixture Xe-Ar is studied at  $x = 0.5$  from 169°K to 400°K. The concentration dependence of  $D_{12}$  is only measured at 295°K. Since the concentration effect on  $D_{12}$  is both small and in agreement with theory we have used calculated values for the concentration dependence at the other temperatures. The results are given in the figs. 41-44 and the tables XVII and XVIII.

j. Xe-Kr.  $D_{12}$  at  $x = 0.5$  is measured from 169°K to 400°K. At 169°K the measurements are less accurate in view of the low value of  $D_{12}$ . Also for this mixture the concentration dependence of  $D_{12}$  is only measured at 295°K. As in the case of Xe-Ar the concentration effect on  $D_{12}$  is both small and in agreement with theory. The results are presented in the figs. 45-48 and the tables XIX and XX.

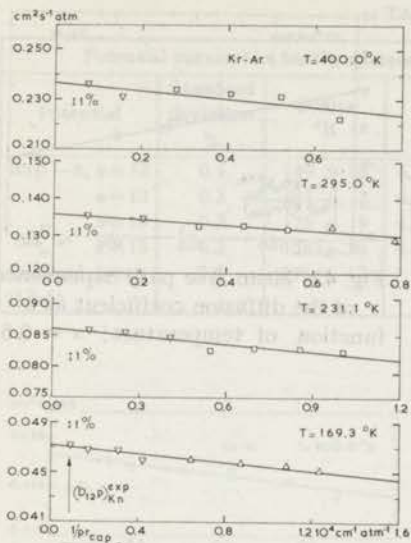


Fig. 36. Mean free path dependence of the diffusion coefficient at different temperatures;  $x = 0.5$ .

- $\nabla$   $r_{\text{cap}} = 0.1372$  cm
- $\square$   $r_{\text{cap}} = 0.1008$  cm
- $\triangle$   $r_{\text{cap}} = 0.0699$  cm

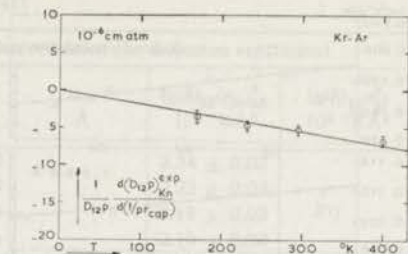


Fig. 37. Mean free path dependence of the diffusion coefficient as a function of temperature;  $x = 0.5$ .

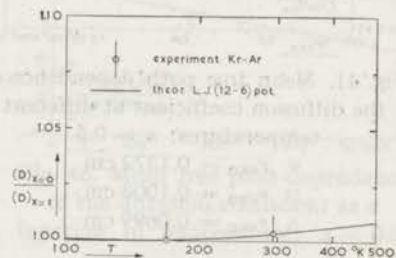


Fig. 39. Concentration dependence of the diffusion coefficient as a function of temperature.

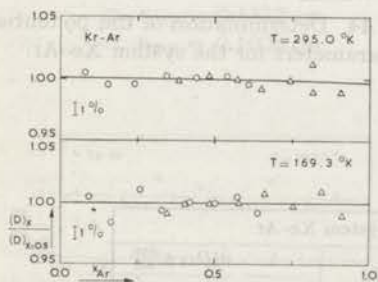


Fig. 38. Concentration dependence of the diffusion coefficient at different temperatures.

- $\circ$  Ar-diffusion run
- $\triangle$  Kr-diffusion run

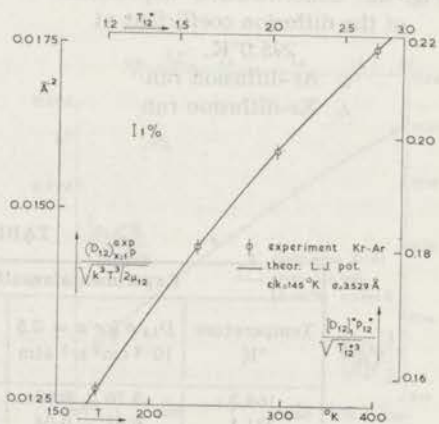


Fig. 40. Determination of the potential parameters for the system Kr-Ar.

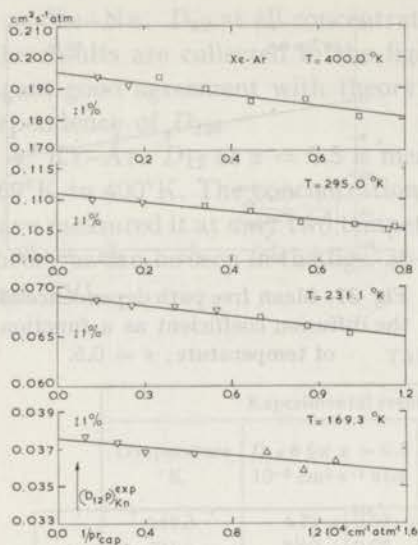


Fig. 41. Mean free path dependence of the diffusion coefficient at different temperatures;  $x = 0.5$ .

- $\nabla$   $r_{\text{cap}} = 0.1372$  cm
- $\square$   $r_{\text{cap}} = 0.1008$  cm
- $\triangle$   $r_{\text{cap}} = 0.0699$  cm

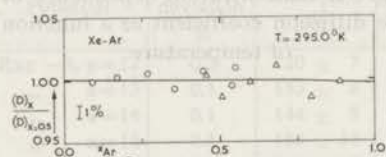


Fig. 43. Concentration dependence of the diffusion coefficient at  $295.0^\circ\text{K}$ .

- $\circ$  Ar-diffusion run
- $\triangle$  Xe-diffusion run

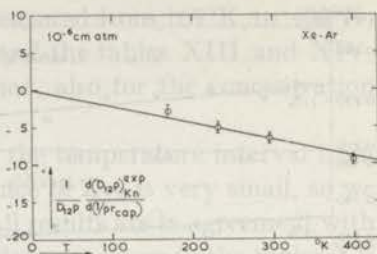


Fig. 42. Mean free path dependence of the diffusion coefficient as a function of temperature;  $x = 0.5$ .

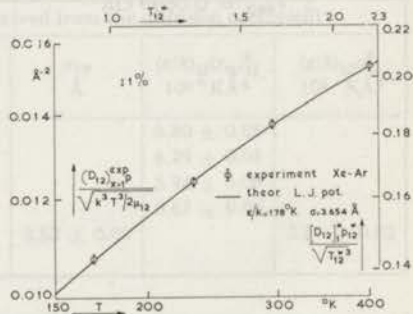


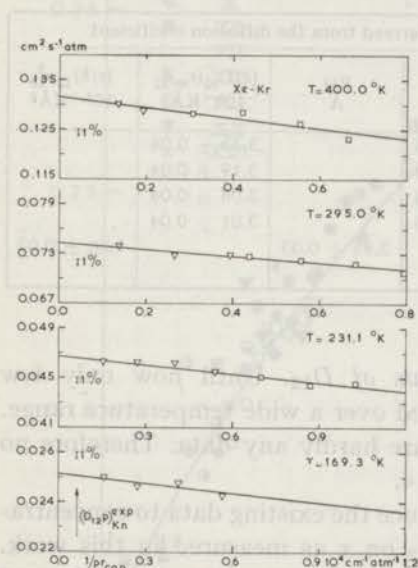
Fig. 44. Determination of the potential parameters for the system Xe-Ar.

TABLE XVII

| Experimental results for the system Xe-Ar |   |                                   |   |
|---|---|-----------------------------------|---|
| Temperature<br>°K                         | $D_{12} \bar{p}$ for $x = 0.5$<br>$10^{-2} \text{ cm}^2 \text{ s}^{-1} \text{ atm}$ | $\frac{(D)_{x=0.5}}{(D)_{x=1.0}}$ | $\frac{1}{D_{12} \bar{p}} \frac{d(D_{12} \bar{p})_{\text{EXP}}}{d(1/\bar{r}_{\text{cap}})}$<br>$10^{-6} \text{ cm atm}$ |
| 169.3                                     | $3.76 \pm 0.03$   | $1.000 \pm 0.001$                 | $-(3.0 \pm 0.7)$  |
| 231.1                                     | $6.91 \pm 0.04$   | $1.001 \pm 0.001$                 | $-(5.1 \pm 0.6)$  |
| 295.0                                     | $11.10 \pm 0.06$  | $1.003 \pm 0.002$                 | $-(6.5 \pm 0.6)$  |
| 400.0                                     | $19.54 \pm 0.12$  | $1.006 \pm 0.003$                 | $-(9.3 \pm 0.6)$  |

TABLE XVIII

| Potential parameters for the system Xe-Ar, derived from the diffusion coefficient |                      |                        |                 |                 |   |  |
|---|----------------------|------------------------|-----------------|-----------------|---|--|
| Potential   | Standard deviation % | $(\epsilon/k)_{12}$ °K | $(r_m)_{12}$ Å  | $\sigma_{12}$ Å | $(\epsilon/k)_{12}(r_m)_{12}^5$ $10^5$ °KÅ <sup>5</sup> | $(\epsilon/k)_{12}\sigma_{12}^5$ $10^5$ °KÅ <sup>5</sup> |
| Exp $-6, \alpha=12$   | 0.4                  | $149 \pm 5$            | $4.36 \pm 0.03$ |                 | $2.34 \pm 0.02$   |  |
| „ $\alpha=13$   | 0.3                  | $161 \pm 7$            | $4.25 \pm 0.04$ |                 | $2.23 \pm 0.02$   |  |
| „ $\alpha=14$   | 0.2                  | $175 \pm 9$            | $4.15 \pm 0.04$ |                 | $2.15 \pm 0.02$   |  |
| „ $\alpha=15$   | 0.3                  | $188 \pm 14$           | $4.07 \pm 0.06$ |                 | $2.10 \pm 0.02$   |  |
| Lennard-Jones (12-6)  | 0.2                  | $178 \pm 12$           |                 | $3.65 \pm 0.05$ |   | $1.16 \pm 0.01$  |

Fig. 45. Mean free path dependence of the diffusion coefficient at different temperatures;  $\alpha = 0.5$ .

$\nabla$   $r_{\text{cap}} = 0.1372$  cm

$\square$   $r_{\text{cap}} = 0.1008$  cm

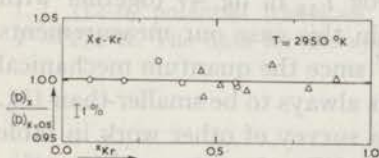


Fig. 47. Concentration dependence of the diffusion coefficient at 295.0 °K.

$\circ$  Kr-diffusion run

$\Delta$  Xe-diffusion run

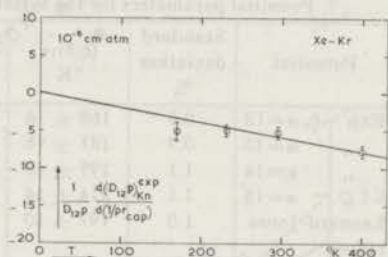
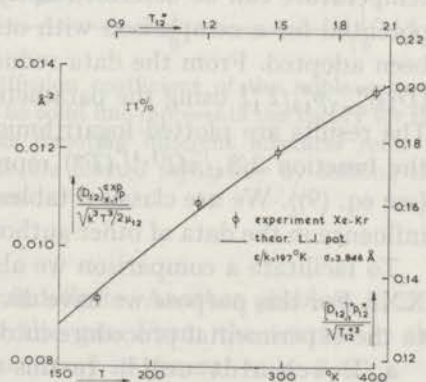
Fig. 46. Mean free path dependence of the diffusion coefficient as a function of temperature;  $\alpha = 0.5$ .

Fig. 48. Determination of the potential parameters for the system Xe-Kr.

TABLE XIX

| Experimental results for the system Xe-Kr |   |                                   |   |
|---|---|-----------------------------------|---|
| Temperature<br>°K                         | $D_{12} p$ for $x = 0.5$<br>$10^{-2} \text{ cm}^2 \text{ s}^{-1} \text{ atm}$ | $\frac{(D)_{x=0.5}}{(D)_{x=1.0}}$ | $\frac{1}{D_{12} p} \frac{d(D_{12} p)_{\text{Kn}}^{\text{exp}}}{d(1/p r_{\text{exp}})}$ |
|   |   |                                   | $10^{-6} \text{ cm atm}$  |
| 169.3                                     | $2.51 \pm 0.03$   | $1.000 \pm 0.000$                 | $-(5.1 \pm 1.1)$  |
| 231.1                                     | $4.68 \pm 0.04$   | $1.000 \pm 0.001$                 | $-(5.0 \pm 0.7)$  |
| 295.0                                     | $7.43 \pm 0.07$   | $1.001 \pm 0.001$                 | $-(5.3 \pm 0.7)$  |
| 400.0                                     | $13.15 \pm 0.12$  | $1.002 \pm 0.002$                 | $-(7.8 \pm 0.7)$  |

TABLE XX

| Potential parameters for the system Xe-Kr, derived from the diffusion coefficient |                         |                           |                   |                    |  |   |
|---|-------------------------|---------------------------|-------------------|--------------------|--|---|
| Potential   | Standard deviation<br>% | $(\epsilon/k)_{12}$<br>°K | $(r_m)_{12}$<br>Å | $\sigma_{12}$<br>Å | $(\epsilon/k)_{12} (r_m)_{12}^5$<br>$10^5 \text{ } ^\circ\text{K} \text{ Å}^5$ | $(\epsilon/k)_{12} \sigma_{12}^5$<br>$10^5 \text{ } ^\circ\text{K} \text{ Å}^5$ |
| Exp -6, $\alpha=12$   | 0.8                     | $168 \pm 6$               | $4.57 \pm 0.03$   |                    | $3.33 \pm 0.04$  |   |
| „ $\alpha=13$   | 0.9                     | $181 \pm 8$               | $4.46 \pm 0.04$   |                    | $3.19 \pm 0.04$  |   |
| „ $\alpha=14$   | 1.1                     | $199 \pm 10$              | $4.34 \pm 0.04$   |                    | $3.08 \pm 0.04$  |   |
| „ $\alpha=15$   | 1.1                     | $214 \pm 14$              | $4.26 \pm 0.05$   |                    | $3.01 \pm 0.04$  |   |
| Lennard-Jones<br>(12-6)   | 1.0                     | $197 \pm 10$              |                   | $3.85 \pm 0.03$    |  | $1.66 \pm 0.02$   |

5. *Comparison with other measurements of  $D_{12}$ .* Until now only few measurements of  $D_{12}$  have been performed over a wide temperature range. Especially at lower temperatures there are hardly any data. Therefore no other work on  $D_{12}$  is reported in section 4.

To make a comparison possible we reduce the existing data to concentration  $x = 1$ , using the dependence of  $D_{12}$  on  $x$  as measured in this work. Obviously in cases where trace amounts of the heavier component are used this procedure is not necessary. As all our results for  $D_{12}$  as a function of temperature can be described fairly well with the Lennard-Jones (12-6) potential for a comparison with other authors the following procedure has been adopted. From the data reduced to  $x = 1$  we determine the quantity  $(D_{12})_{x=1}^* p_{12}^* / T_{12}^{*3/2}$  using the parameters as obtained in this work in section 4. The results are plotted logarithmically *vs.*  $\log T_{12}^*$  in fig. 49 together with the function  $3/8 \sqrt{\pi} \Omega^{(1,1)}(T^*)$  representing in this case our measurements (see eq. (9)). We use classical tables of  $\Omega^{(1,1)}$  since the quantum mechanical influence in the data of other authors appears always to be smaller than 1%.

To facilitate a comparison we also make a survey of other work in table XXI. For this purpose we have divided the diffusion experiments according to the experimental procedure into four groups:

a. *Loschmidt cell*<sup>8)</sup>. In this type of apparatus the rate of change in concentration along a tube is studied. Usually the tube is separated into two identical parts which can be isolated from each other. In most cases



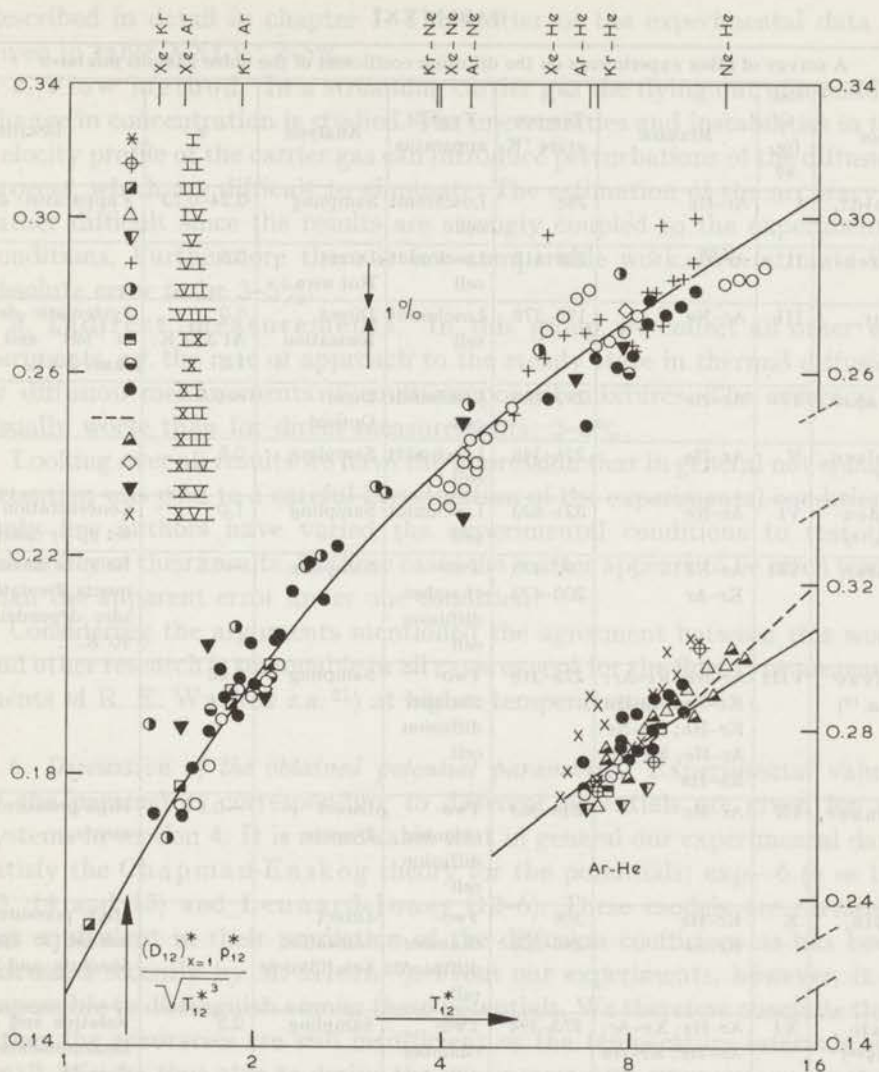


Fig. 49. A survey of other work on the diffusion coefficient of the noble gaseous mixtures. The symbols refer to table XXI. The solid line represents the theory for the L.J. (12-6) potential (classical). The marks denoting different mixtures refer to  $T = 273^\circ\text{K}$ . The data for the system Ar-He are plotted separately by shifting the ordinate.

the starting point of a diffusion run is indefinite. Another problem in this apparatus is to avoid a convection of the gas. From the scatter in the experiments we estimate the absolute accuracy in general to be 2-5%.

b. Two-chamber diffusion cell. This method, introduced by Ney and Armistead<sup>9</sup>), is also used in this work. The problems arising have been

TABLE XXI

| A survey of other experiments on the diffusion coefficient of the noble gaseous mixtures |                 |   |                   |                            |                                    |                         |   |
|--|-----------------|---|-------------------|----------------------------|------------------------------------|-------------------------|---|
| Author   | Ref. to fig. 49 | Mixture   | Temperature °K    | Type of apparatus          | Analysis                           | $\alpha$                | Details   |
| R. Schmidt, <i>e.a.</i> <sup>10)</sup>   | I               | Ar-He   | 288               | Loschmidt cell             | Sampling                           | 0.24-0.73               | 2 apparatus: $\Delta \approx 1.5\%$                             |
| R. A. Strehlow <sup>11)</sup>  | II              | Ar-He   | 288-418           | Loschmidt cell             | Direct Hot wire                    | 0.5                     |   |
| I. Amdur, <i>e.a.</i> <sup>12)</sup>   | III             | Ar-Xe   | 195-378           | Loschmidt cell             | Direct Ionization                  | 0.0<br>At 330°K:<br>1.0 | Systematic deviations in "left" and "right" runs: 2-6%          |
| B. A. Ivakin, <i>e.a.</i> <sup>13)</sup>   | IV              | Ar-He   | 287-465           | Loschmidt cell             | Direct Optical                     | $\sim 0.5$              |   |
| J. N. Holsen, <i>e.a.</i> <sup>14)</sup>   | V               | Ar-He   | 276-346           | Loschmidt cell             | Sampling                           | 0.5                     |   |
| J. Freudenthal, <i>e.a.</i> <sup>15)</sup>   | VI              | Ar-Ne   | 321-623           | Loschmidt cell             | Sampling                           | 1.0                     | Concentration gradient set up by cataphoresis.                  |
| K. Schäfer, <i>e.a.</i> <sup>16)</sup>   | VII             | Ar-Ne<br>Kr-Ar  | 90-473<br>200-473 | Two-chamber diffusion cell | Sampling                           | $\sim 0.5$              | Relative measurements. Deviating pressure dependence at 90°K.   |
| B.N. Srivastava, <i>e.a.</i> <sup>17)</sup>  | VIII            | Ar-Ne; Kr-Ar;<br>Kr-Ne; Ne-He;<br>Kr-He; Xe-Ne;<br>Ar-He; Xe-Ar;<br>Xe-He | 273-318           | Two-chamber diffusion cell | Sampling                           | 0.63                    |   |
| I.F. Golubev, <i>e.a.</i> <sup>18)</sup>   | IX              | Ar-He   | 298-363           | Two-chamber diffusion cell | Direct Density                     | $\sim 0.5$              | High pressure experiments.                                      |
| L. Durbin, <i>e.a.</i> <sup>19)</sup>  | X               | Kr-He<br>Kr-Ar  | 308<br>248-308    | Two-chamber diffusion cell | Direct Ionization<br>Scintillation | --                      | High pressure experiments; 2 apparatus: absolute and relative.  |
| A. P. Malinauskas <sup>20)</sup>   | XI              | Ar-He; Xe-Ar;<br>Xe-He; Kr-He<br>Kr-Ar; Xe-Kr                             | 273-394           | Two-chamber diffusion cell | Sampling                           | 0.5                     | Relative and absolute measurements: $\Delta \approx 2\%$ .      |
| R. E. Walker, <i>e.a.</i> <sup>21)</sup>   | XII             | Ar-He   | 300-1100          | Flow method                | Sampling                           | 0.0<br>At 298°K:<br>1.0 | Point source technique.   |
| J. C. Giddings, <i>e.a.</i> <sup>22)</sup>   | XIII            | Ar-He   | 296-498           | Flow method                | Sampling                           | 1.0                     | Chromatographic technique.                                      |
| B. N. Srivastava, <i>e.a.</i> <sup>23)</sup>   | XIV             | Kr-He<br>Kr-Ne; Kr-Ar   | 305<br>302        | Multi-component diffusion  | Direct Scintillation               | 1.0                     | Two-chamber diffusion cell.                                     |
| H. Watts <sup>24)</sup>  | XV              | Kr-He; Kr-Ne;<br>Kr-Ar; Xe-He;<br>Xe-Ne; Xe-Ar;<br>Xe-Kr                  | 303               | Multi-component diffusion  | Direct Geiger-Müller counter       | 1.0                     | Two-chamber diffusion cell; 2 apparatus: $\Delta \approx 4\%$ . |
| S. C. Saxena, <i>e.a.</i> <sup>25)</sup>   | XVI             | Ar-He   | 251-418           | Thermal diffusion          | Direct Ionization                  | 1.0                     | Also ordinary diffusion; 2 apparatus: $\Delta \approx 4\%$ .    |

described in detail in chapter I. The scatter of the experimental data as given in table XXI is: 2-5%.

c. Flow method. In a streaming carrier gas the dying out of a sudden change in concentration is studied. The uncertainties and instabilities in the velocity profile of the carrier gas can introduce perturbations of the diffusion process, which are difficult to eliminate. The estimation of the accuracy is rather difficult since the results are strongly coupled to the experimental conditions. Furthermore there is few comparable work. We estimate the absolute error to be 3-5%.

d. Indirect measurements. In this group we collect all other experiments, *e.g.* the rate of approach to the steady state in thermal diffusion or diffusion measurements in multicomponent mixtures. The accuracy is usually worse than for direct measurements: 3-5%.

Looking over all results we have the impression that in general not enough attention was paid to a careful investigation of the experimental conditions. Only few authors have varied the experimental conditions to test the reliability of their results. In those cases the scatter appears to be often worse than the apparent error under one condition.

Considering the arguments mentioned the agreement between this work and other research is reasonable in all cases except for the flow-type measurements of R. E. Walker *e.a.*<sup>21)</sup> at higher temperatures.

6. *Discussion of the obtained potential parameters.* Experimental values of the parameters corresponding to different potentials are given for all systems in section 4. It is remarkable that in general our experimental data satisfy the Chapman-Enskog theory for the potentials: exp-6 ( $\alpha = 12, 13, 14$  and  $15$ ) and Lennard-Jones (12-6). These models are certainly not equivalent in their prediction of the diffusion coefficient as has been discussed recently by M. Klein<sup>26)</sup>. From our experiments, however, it is impossible to distinguish among these potentials. We therefore conclude that either the accuracies are still insufficient or the temperature intervals too small. We are thus able to derive the parameters with respect to more than one potential.

If one can apply several potential models to describe the experiments of a particular mixture one expects a definite relation between the obtained parameters. As a check on our results we shall investigate this aspect in some detail.

The relation between the parameters for two potentials which are nearly equivalent in the description of  $D_{12}$  of a mixture is given by the relative positions of the curves  $\log \Omega^{(1,1)*}$  vs.  $\log T^*$  (see eq. (9)). This relation is not unique, it depends on the intervals in the reduced temperatures for which the comparison will be made. Let us characterize the intervals in the following way: for the extension of the interval we take ratio,  $T_{\max}^*/T_{\min}^*$  and for

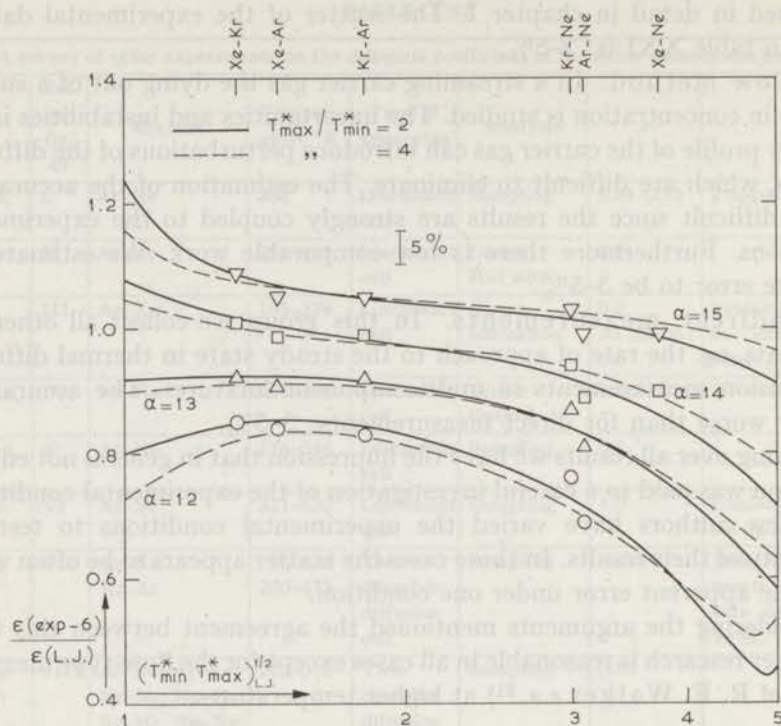


Fig. 50. The parameter ratios  $\varepsilon(\text{exp-6})/\varepsilon(\text{L.J.})$  for the diffusion coefficients for different values of  $\alpha$ .

- $\nabla$  experiment,  $\alpha = 15$        $\square$  experiment,  $\alpha = 14$   
 $\triangle$  experiment,  $\alpha = 13$        $\circ$  experiment,  $\alpha = 12$

the position of the interval:  $(T_{\min}^* T_{\max}^*)^{\frac{1}{2}}$ . The last choice is suggested by the fact that in this way  $(T_{\min}^* T_{\max}^*)^{\frac{1}{2}}$  corresponds to the mean value of  $\log T^*$ . For a fixed value of  $T_{\max}^*/T_{\min}^*$  we have derived the relation between different potentials as a function of  $(T_{\min}^* T_{\max}^*)^{\frac{1}{2}}$  in the following way. At various values of  $(T_{\min}^* T_{\max}^*)^{\frac{1}{2}}$  we have fitted the curve  $\log \Omega^{(1,1)}$  vs.  $\log T^*$  for the Lennard-Jones (12-6) potential to the corresponding curve for the (exp-6) potential ( $\alpha = 12, 13, 14$  or  $15$ ). From the shifts in the axis necessary to obtain the best agreement of the curves within an interval of magnitude  $T_{\max}^*/T_{\min}^* = 2$ , one derives the ratios of  $\varepsilon$ - and  $\sigma(r_m)$ -values belonging to both potentials. The same procedures have also been performed for an extension of the interval  $T_{\max}^*/T_{\min}^* = 4$ . The results of these procedures are shown in the figs. 50 and 51; the heavy and dashed lines correspond to  $T_{\max}^*/T_{\min}^* = 2$  and  $4$ , respectively. One notes that the magnitudes of the reduced temperature interval do not influence the results too much. As in this work  $T_{\max}^*/T_{\min}^*$  for all mixtures vary from 2.5 to 4 a significant comparison can be made between the curves and the ratios of the

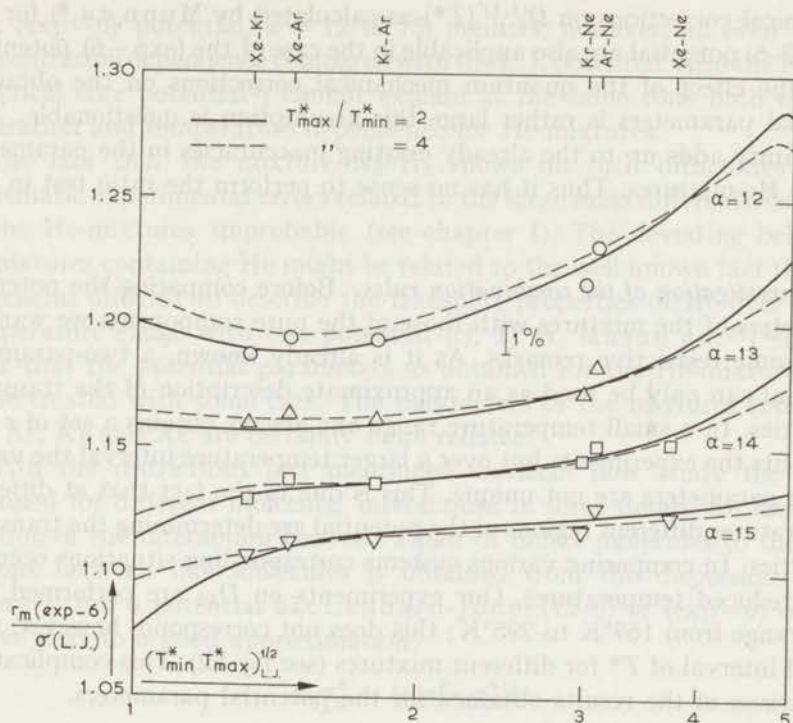


Fig. 51. The parameter ratios  $r_m(\text{exp-6})/\sigma$  (L.J.) for the diffusion coefficients for different values of  $\alpha$ .

- $\nabla$  experiment,  $\alpha = 15$        $\square$  experiment,  $\alpha = 14$   
 $\triangle$  experiment,  $\alpha = 13$        $\circ$  experiment,  $\alpha = 12$

potential parameters obtained in section 4. The ratios  $\varepsilon(\text{exp-6})/\varepsilon(\text{L.J.})$  or  $r_m(\text{exp-6})/\sigma(\text{L.J.})$  obtained for different mixtures should be in between both curves in the figs. 50 and 51. Considering the experimental accuracies in  $\varepsilon$  ( $\sim 5\%$ ) and in  $\sigma$  or  $r_m$  ( $\sim 1\%$ ) the data satisfy this condition quite well. We may therefore conclude that the shifting procedure used in section 4 is self-consistent.

We have restricted these considerations to mixtures behaving almost classically. The quantum mechanical corrections to be applied to  $\Omega^{(1,1)^*}(T^*)$  for the mixtures containing He are determined by the quantum parameter  $A^* = h/\sigma_{12}\sqrt{2\mu_{12}\varepsilon_{12}}$ . For each mixture, corresponding to another value of  $A^*$ , different  $\Omega^{(1,1)^*}(T^*)$ -functions are obtained, so the procedures as sketched in the figs. 50 and 51 in general lead to different curves for each mixture. Thus the afore mentioned comparison between mixtures cannot be extended for mixtures containing He. In addition we may note that for the (exp-6) potential  $\Omega^{(1,1)^*}(T^*)$  has not been calculated independently as a function of  $A^*$ ; in section 3 we have therefore assumed that the quantum

mechanical corrections on  $\Omega^{(1,1)^*}(T^*)$  as calculated by Munn *e.a.*<sup>6)</sup> for the L.J. (12-6) potential are also applicable in the case of the (exp-6) potential. Since the effect of the quantum mechanical corrections on the obtained potential parameters is rather large this assumption is questionable. This uncertainty adds up to the already existing inaccuracies in the parameters for the He-mixtures. Thus it has no sense to perform the ratio test in this case.

7. *Investigation of the combination rules.* Before comparing the potential parameters of the mixtures with those of the pure components we want to make some restrictive remarks. As it is already known, a two-parameter potential can only be used as an approximate description of the transport properties. In a small temperature range one always obtains a set of  $\epsilon$  and  $\sigma$  that fits the experiments but over a larger temperature interval the values for the parameters are not unique. This is due to the fact that at different temperatures different regions of the potential are determining the transport properties. In comparing various systems corresponding situations occur at equal reduced temperatures. Our experiments on  $D_{12}$  are performed in a fixed range from 169°K to 295°K; this does not correspond, however, with a fixed interval of  $T^*$  for different mixtures (see fig. 52). This complicates a comparison of the results obtained for the potential parameters.

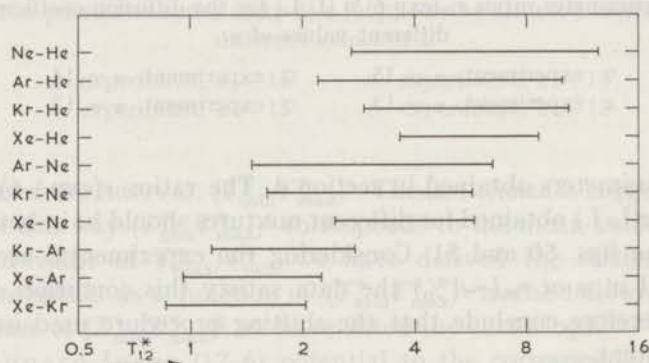


Fig. 52. Temperature ranges reduced with respect to  $\epsilon_{12}$  (L.J.).

A second remark refers to the deviating concentration dependence of the mixtures containing He. For these mixtures the concentration dependence is larger than predicted from theory for the L.J. (12-6) potential, although the shapes of the curves agree. This is probably not due to the exclusion of the higher approximations of the diffusion coefficient since the Sonine expansion converges very rapidly. This can be seen from calculations by E. A. Mason<sup>4)</sup> in limiting cases such as a Lorentzian and a quasi-Lorentzian gas. We have therefore investigated other potential models.

The (exp-6) potential,  $\alpha = 12$  to 15, predicts, however, an even smaller concentration dependence compared with the L.J. potential. Also the Kihara spherical core potential<sup>5)</sup> cannot explain at the same time both the concentration and temperature dependence for He-mixtures.

The fact that the mixture N<sub>2</sub>-H<sub>2</sub> shows no such difficulties makes systematic experimental errors related to the large mass difference occurring in the He-mixtures improbable (see chapter I). The deviating behaviour of mixtures containing He might be related to the well known fact that it is in general difficult to describe the transport properties of He over a large temperature range with one potential (*cf.* E. A. Mason *e.a.*<sup>27)28)</sup>). It is clear that the potential parameters as obtained for the He-mixtures have to be treated with some care. The parameters of the mixtures containing Ne, Ar, Kr and Xe are certainly more reliable.

With the restrictions just mentioned we shall now study the results obtained for different molecular interactions in some detail. An important relation of the interaction between a pair of unlike molecules to the interactions between like molecules is obtained from the dispersion energy theory<sup>3)</sup>. For a potential like Lennard-Jones (12-6) or (exp-6) one can derive that to a good approximation:

$$\epsilon_{ij}\sigma_{ij}^6 = \{\epsilon_{ii}\sigma_{ii}^6\epsilon_{jj}\sigma_{jj}^6\}^{\frac{1}{2}}. \quad (10)$$

The subscripts  $i$  and  $j$  refer to different species of molecules. Usually one combines the arguments from dispersion forces with the assumption that the molecular repulsion is fairly well described by regarding the molecules as hard spheres of diameter  $\sigma$ . In this case one gets:

$$\sigma_{ij} = \frac{1}{2}(\sigma_{ii} + \sigma_{jj}). \quad (11)$$

As far as different molecules do not differ much in size one obtains from (10) and (11):

$$\epsilon_{ij} = (\epsilon_{ii}\epsilon_{jj})^{\frac{1}{2}}. \quad (12)$$

When there are sufficient combinations of mixed parameters available one can test the combination rules without invoking the knowledge of the parameters for the pure components in the following way. For all mixtures containing the gases  $i$ ,  $j$  and  $k$  the rules (10), (11) and (12) can be written as:

$$\epsilon_{ii}\sigma_{ii}^6 = \frac{\epsilon_{ij}\sigma_{ij}^6\epsilon_{jk}\sigma_{jk}^6}{\epsilon_{jk}\sigma_{jk}^6} \quad (13)$$

$$\sigma_{ii} = \sigma_{ij} + \sigma_{ik} - \sigma_{jk} \quad (14)$$

$$\epsilon_{ii} = \frac{\epsilon_{ij}\epsilon_{ik}}{\epsilon_{jk}}. \quad (15)$$

By interchanging the subscripts similar expressions are obtained for the

TABLE XXII

| Test of the combination rules of the L.J. (12-6) potential parameters for the mixed interactions of the noble gas atoms |  |   |  |  |  |  |
|---|--|---|--|--|--|--|
| Binary mixture constituents   | potential parameters   | Calculated potential parameters for the pure components from eqs. (13), (14) and (15) |  |  |  |  |
|   |  | He  | Ne   | Ar   | Kr   | Xe   |
| He-Ne-Ar  | $\epsilon/k$ °K<br>$\sigma$ Å<br>$(\epsilon/k)\sigma^6$ °KÅ <sup>6</sup>   | 15.4 ± 2<br>2.51 ± 0.04<br>(4.12 ± 0.26) 10 <sup>3</sup>                              | 36.4 ± 5<br>2.77 ± 0.04<br>(1.56 ± 0.10) 10 <sup>4</sup> | 105 ± 13<br>3.45 ± 0.04<br>(1.94 ± 0.12) 10 <sup>5</sup> |  |  |
| He-Ne-Kr  | $\epsilon/k$ °K<br>$\sigma$ Å<br>$(\epsilon/k)\sigma^6$ °KÅ <sup>6</sup>   | 13.2 ± 2<br>2.57 ± 0.06<br>(4.00 ± 0.34) 10 <sup>3</sup>                              | 42.4 ± 7<br>2.71 ± 0.06<br>(1.60 ± 0.14) 10 <sup>4</sup> |  | 115 ± 20<br>3.77 ± 0.06<br>(4.05 ± 0.34) 10 <sup>5</sup> |  |
| He-Ne-Xe  | $\epsilon/k$ °K<br>$\sigma$ Å<br>$(\epsilon/k)\sigma^6$ °KÅ <sup>6</sup>   | 15.9 ± 4<br>2.53 ± 0.08<br>(4.48 ± 0.45) 10 <sup>3</sup>                              | 35.2 ± 8<br>2.75 ± 0.08<br>(1.43 ± 0.15) 10 <sup>4</sup> |  |  | 136 ± 30<br>4.21 ± 0.08<br>(1.04 ± 0.11) 10 <sup>6</sup> |
| He-Ar-Kr  | $\epsilon/k$ °K<br>$\sigma$ Å<br>$(\epsilon/k)\sigma^6$ °KÅ <sup>6</sup>   | 10.8 ± 2<br>2.62 ± 0.06<br>(4.05 ± 0.29) 10 <sup>3</sup>                              |  | 149 ± 25<br>3.34 ± 0.06<br>(1.97 ± 0.14) 10 <sup>5</sup> | 141 ± 24<br>3.72 ± 0.06<br>(3.99 ± 0.29) 10 <sup>5</sup> |  |
| He-Ar-Xe  | $\epsilon/k$ °K<br>$\sigma$ Å<br>$(\epsilon/k)\sigma^6$ °KÅ <sup>6</sup>   | 10.5 ± 2<br>2.70 ± 0.09<br>(4.66 ± 0.40) 10 <sup>3</sup>                              |  | 154 ± 32<br>3.26 ± 0.09<br>1.75 ± 0.16) 10 <sup>5</sup>  |  | 206 ± 43<br>4.04 ± 0.09<br>(1.03 ± 0.09) 10 <sup>6</sup> |
| He-Kr-Xe  | $\epsilon/k$ °K<br>$\sigma$ Å<br>$(\epsilon/k)\sigma^6$ °KÅ <sup>6</sup>   | 9.2 ± 3<br>2.69 ± 0.09<br>(4.31 ± 0.46) 10 <sup>3</sup>                               |  |  | 165 ± 40<br>3.65 ± 0.09<br>(3.75 ± 0.40) 10 <sup>5</sup> | 235 ± 60<br>4.05 ± 0.09<br>(1.08 ± 0.12) 10 <sup>6</sup> |
| Ne-Ar-Kr  | $(\epsilon/k)$ °K<br>$\sigma$ Å<br>$(\epsilon/k)\sigma^6$ °KÅ <sup>6</sup> |   | 29.7 ± 3<br>2.82 ± 0.05<br>(1.58 ± 0.04) 10 <sup>4</sup> | 128 ± 11<br>3.40 ± 0.05<br>(1.91 ± 0.05) 10 <sup>5</sup> | 164 ± 15<br>3.66 ± 0.05<br>(4.11 ± 0.10) 10 <sup>5</sup> |  |
| Ne-Ar-Xe  | $\epsilon/k$ °K<br>$\sigma$ Å<br>$(\epsilon/k)\sigma^6$ °KÅ <sup>6</sup>   |   | 24.0 ± 4<br>2.94 ± 0.08<br>(1.58 ± 0.07) 10 <sup>4</sup> | 159 ± 23<br>3.28 ± 0.08<br>(1.91 ± 0.09) 10 <sup>5</sup> |  | 199 ± 26<br>4.02 ± 0.08<br>(0.94 ± 0.04) 10 <sup>6</sup> |
| Ne-Kr-Xe  | $\epsilon/k$ °K<br>$\sigma$ Å<br>$(\epsilon/k)\sigma^6$ °KÅ <sup>6</sup>   |   | 24.5 ± 4<br>2.87 ± 0.06<br>(1.54 ± 0.08) 10 <sup>4</sup> |  | 199 ± 26<br>3.61 ± 0.06<br>(4.20 ± 0.20) 10 <sup>5</sup> | 195 ± 25<br>4.09 ± 0.06<br>(0.97 ± 0.05) 10 <sup>6</sup> |
| Ar-Kr-Xe  | $\epsilon/k$ °K<br>$\sigma$ Å<br>$(\epsilon/k)\sigma^6$ °KÅ <sup>6</sup>   |   |  | 131 ± 16<br>3.33 ± 0.08<br>(1.87 ± 0.07) 10 <sup>5</sup> | 161 ± 20<br>3.73 ± 0.08<br>(4.22 ± 0.14) 10 <sup>5</sup> | 242 ± 30<br>3.97 ± 0.08<br>(0.96 ± 0.04) 10 <sup>6</sup> |
| Mean values   | $(\epsilon/k)\sigma^6$ °KÅ <sup>6</sup>                                    | (4.24 ± 0.17) 10 <sup>3</sup>   | (1.56 ± 0.03) 10 <sup>4</sup>                            | (1.90 ± 0.04) 10 <sup>5</sup>                            | (4.10 ± 0.08) 10 <sup>5</sup>                            | (0.98 ± 0.03) 10 <sup>6</sup>                            |
| Mean values from other sources  | $\epsilon/k$ °K<br>$\sigma$ Å<br>$(\epsilon/k)\sigma^6$ °KÅ <sup>6</sup>   | 10.5<br>2.56<br>2.95 10 <sup>3</sup>  | 35.9<br>2.77<br>1.62 10 <sup>4</sup>                     | 121<br>3.42<br>1.93 10 <sup>5</sup>                      | 173<br>3.63<br>3.95 10 <sup>5</sup>                      | 218<br>4.05<br>0.96 10 <sup>6</sup>                      |



pure gases  $j$  and  $k$ . As in this work we have utilized five pure gases,  $\epsilon_{ij}$  and  $\sigma_{ij}$  are overdetermined, so this method enables a direct test of the combination rules. To see this we arrange the different systems in groups containing binary mixtures of only three pure gases, *e.g.* Ne-He, Ar-He and Ar-Ne. From eqs. (13), (14) and (15) we calculate in each group the parameters of the pure constituents: He, Ne and Ar in this example. The 5 pure gases give rise to 10 groups of three binary mixtures, each gas appearing in 6 different groups. So one obtains 6 sets of parameters that have to be constant when the combination rules hold. Furthermore the resulting values must agree with the parameters obtained from other sources. The procedure is worked out in table XXII for the L.J. (12-6) potential. In order to obtain a maximum of accuracy the values of  $(\epsilon/k) \sigma^6$  are calculated from the experimental data of  $(\epsilon/k) \sigma^a$  and  $\sigma$  instead of  $\epsilon/k$  and  $\sigma$ . The validity of the combination rules can be concluded from a comparison of the data along a column. One sees that only the combination rule for  $(\epsilon/k) \sigma^6$  (see eq. (10)) holds within the limits of the accuracy.

The mean value of  $(\epsilon/k) \sigma^6$  for all pure gases is reported in the last but one row. These values can be compared with the data from other sources. We therefore have averaged the data from the survey of Hirschfelder, *e.a.*<sup>3)</sup> and from refs. 27 and 29 to 35. The agreement with our results is good in all cases except for He. The deviating behaviour of He is discussed earlier in this section. But even if we restrict the comparison of the potential parameters to the gases Ne, Ar, Kr and Xe the conclusions for the validity of the combination rules remain the same. Although in this case also the rules (11) and (12) are satisfied just within the experimental accuracy the agreement with the data from other sources is too poor.

Similar calculations are performed for the (exp-6) potential,  $\alpha = 12, 13, 14$  and  $15$ , as far as these models fit the experiments. The comparison is only made at a fixed value of  $\alpha$  in order to preserve a two-parameter model. The rules (10) and (11) are tested with respect to  $r_m$  i.s.o.  $\sigma$ . We also have tested the following expression that is often used for this potential:

$$\left(\frac{1}{r_m}\right)_{ij} = \frac{1}{2} \left\{ \left(\frac{1}{r_m}\right)_{ii} + \left(\frac{1}{r_m}\right)_{jj} \right\}. \quad (16)$$

This rule can be derived from the repulsive part of the (exp-6) potential<sup>36)</sup>. As in the case of the L.J. potential none of the combination rules hold except the rule (10) for  $(\epsilon/k)(r_m)^6$ . We report the final results from this rule in table XXIII. A comparison with the data of  $(\epsilon/k)(r_m)^6$  from other sources is somewhat more difficult since different authors use different values of  $\alpha$  to describe their experiments (see refs. 27, 32 and 37 to 44). Treating our results as a function of  $\alpha$  we conclude to a good agreement for all gases with the exception again of He.

TABLE XXIII

| Results from combination rule (13) for the (exp-6) potential |           |                       |                              |                 |                       |                                     |  |
|--|-----------|-----------------------|------------------------------|-----------------|-----------------------|-------------------------------------|--|
| Gas  | This work |                       |                              | From literature |                       |                                     |  |
|  | $\alpha$  | $(\epsilon/k)(r_m)^6$ | $^\circ\text{K}\text{\AA}^6$ | $\alpha$        | $(\epsilon/k)(r_m)^6$ | $^\circ\text{K}\text{\AA}^6$        | Ref.   |
| He   | 12        | —                     | —                            | 12.4            | 8.69                  | $10^3$                              | E. A. Mason, <i>e.a.</i> <sup>27)</sup>      |
|  | 13        | $(7.01 \pm 0.80)$     | $10^3$                       | 12.4            | 7.96                  | $10^3$                              | J. E. Kilpatrick, <i>e.a.</i> <sup>37)</sup> |
|  | 14        | $(7.54 \pm 0.35)$     | $10^3$                       |                 |                       |                                     |  |
|  | 15        | $(7.83 \pm 0.30)$     | $10^3$                       |                 |                       |                                     |  |
| Ne   | 12        | $(3.90 \pm 0.12)$     | $10^4$                       | 13.6            | 3.70                  | $10^4$                              | J. Corner <sup>38)</sup>                     |
|  | 13        | $(3.59 \pm 0.12)$     | $10^4$                       | 14.5            | 3.69                  | $10^4$                              | E. A. Mason, <i>e.a.</i> <sup>27)</sup>      |
|  | 14        | $(3.21 \pm 0.07)$     | $10^4$                       | 14.6            | 3.64                  | $10^4$                              | K. P. Srivastava <sup>39)</sup>              |
|  | 15        | $(3.11 \pm 0.06)$     | $10^4$                       | 15              | 3.21                  | $10^4$                              | G. A. Nicholson, <i>e.a.</i> <sup>40)</sup>  |
| Ar   | 12        | $(4.60 \pm 0.09)$     | $10^5$                       | 13.9            | 4.12                  | $10^5$                              | J. Corner <sup>38)</sup>                     |
|  | 13        | $(4.23 \pm 0.09)$     | $10^5$                       | 14              | 4.12                  | $10^5$                              | E. A. Mason, <i>e.a.</i> <sup>27)</sup>      |
|  | 14        | $(4.06 \pm 0.08)$     | $10^5$                       | 14              | 3.67                  | $10^5$                              | S. C. Saxena, <i>e.a.</i> <sup>41)</sup>     |
|  | 15        | $(3.82 \pm 0.07)$     | $10^5$                       | 14              | 4.12                  | $10^5$                              | M. P. Madan <sup>42)</sup>                   |
|  |           |                       |                              | 14.2            | 3.83                  | $10^5$                              | K. P. Srivastava <sup>39)</sup>              |
|  |           |                       |                              | 15              | 3.86                  | $10^5$                              | E. Whalley, <i>e.a.</i> <sup>43)</sup>       |
|  |           |                       | 17                           | 3.44            | $10^5$                | R. Paul, <i>e.a.</i> <sup>44)</sup> |  |
| Kr   | 12        | $(1.01 \pm 0.02)$     | $10^6$                       | 12              | 0.98                  | $10^6$                              | E. Whalley, <i>e.a.</i> <sup>43)</sup>       |
|  | 13        | $(0.94 \pm 0.02)$     | $10^6$                       | 12              | 0.88                  | $10^6$                              | M. P. Madan <sup>42)</sup>                   |
|  | 14        | $(0.88 \pm 0.02)$     | $10^6$                       | 12              | 0.91                  | $10^6$                              | E. A. Mason <sup>32)</sup>                   |
|  | 15        | $(0.83 \pm 0.02)$     | $10^6$                       | 13              | 0.88                  | $10^6$                              | E. A. Mason <sup>32)</sup>                   |
|  |           |                       |                              | 13.1            | 0.94                  | $10^6$                              | K. P. Srivastava <sup>39)</sup>              |
|  |           |                       |                              | 13.5            | 0.87                  | $10^6$                              | E. A. Mason <sup>32)</sup>                   |
|  |           |                       |                              | 14              | 0.84                  | $10^6$                              | E. A. Mason <sup>32)</sup>                   |
|  |           |                       |                              | 15              | 0.81                  | $10^6$                              | E. A. Mason <sup>32)</sup>                   |
|  |           |                       |                              | 15              | 0.71                  | $10^6$                              | E. Whalley, <i>e.a.</i> <sup>43)</sup>       |
|  |           |                       | 16.1                         | 0.83            | $10^6$                | R. Paul, <i>e.a.</i> <sup>44)</sup> |  |
| Xe   | 12        | $(2.28 \pm 0.07)$     | $10^6$                       | 12              | 2.38                  | $10^6$                              | E. Whalley, <i>e.a.</i> <sup>43)</sup>       |
|  | 13        | $(2.14 \pm 0.07)$     | $10^6$                       | 13              | 1.76                  | $10^6$                              | E. A. Mason, <i>e.a.</i> <sup>27)</sup>      |
|  | 14        | $(2.06 \pm 0.06)$     | $10^6$                       | 13              | 2.16                  | $10^6$                              | K. P. Srivastava <sup>39)</sup>              |
|  | 15        | $(1.99 \pm 0.05)$     | $10^6$                       | 14              | 2.15                  | $10^6$                              | E. Whalley, <i>e.a.</i> <sup>43)</sup>       |
|  |           |                       |                              | 15              | 2.12                  | $10^6$                              | E. Whalley, <i>e.a.</i> <sup>43)</sup>       |
|  |           |                       |                              | 16              | 1.88                  | $10^6$                              | R. Paul, <i>e.a.</i> <sup>44)</sup>          |

For the interaction between helium and the noble gas atoms information is recently available from molecular beam scattering experiments<sup>45)</sup>. Although the accuracy in  $\epsilon_{12}$  and  $\sigma_{12}$  is rather poor one obtains values for  $\epsilon_{12}\sigma_{12}^6$  that have an accuracy of around 10%. The results for  $\epsilon_{12}\sigma_{12}^6$  are systematically 10–20% lower than our values obtained from  $D_{12}$ . This discrepancy will be related to the rather approximate nature of a simple potential model like the Lennard-Jones one.

It is surprising that contrary to the rather common opinion only the combination rule for  $\epsilon_{12}\sigma_{12}^6$  (eq. (10)) appears to be valid. Although the simple rules for  $\epsilon_{12}$  and  $\sigma_{12}$  (eqs. (11) and (12)) cannot strictly be justified on the basis of theory, they are normally believed to have been proved empirically. This paradox can be explained as follows. Due to the lack of relevant measurements for many systems over a large temperature range

an intensive test as performed in this work could not be done earlier. So one usually has treated the problem in the reverse way: one has calculated  $D_{12}$  or another transport property of a mixture from the corresponding Chapman-Enskog expression by assuming that the simple combination rules for  $\epsilon_{12}$  and  $\sigma_{12}$  hold. Apart from thermal diffusion the value of a transport property is far more sensitive to  $\sigma$  than to  $\epsilon$ . At a fixed temperature a comparatively large variation in  $\epsilon$  can easily be compensated by a small change in  $\sigma$ . Furthermore the values of  $\sigma$  for pure gases do not differ much, so the exact form of the combination rule for  $\sigma_{12}$  is not too important. As a result the calculation can in general be brought in agreement with the experiments by making use of the freedom that remains in the choice of  $\epsilon$  and  $\sigma$  for the pure components. This limits the practical consequences of the failure of the simple combination rules found in this work.

The fact that the only combination rule that can easily be derived from theory has been proved to be valid experimentally, is a strong argument in favour of the physical reality of such simple potential models as the Lennard-Jones and (exp-6) potential.

#### REFERENCES

1. Van Heijningen, R. J. J., Feberwee, A., van Oosten, A. and Beenakker, J. J. M., *Physica* **32** (1966) 1649.
2. Chapman, S. and Cowling, T. G., *The Mathematical Theory of Non-Uniform Gases* (Cambridge University Press, New York, 1952).
3. Hirschfelder, J. O., Curtiss, C. F. and Bird, R. B., *The Molecular Theory of Gases and Liquids* (John Wiley and Sons, Inc., New York, 1964).
4. Mason, E. A., *J. chem. Phys.* **27** (1957) 75; 782.
5. Kihara, T., *Imperfect Gases* (Asakura Bookstore, Tokyo, 1949); *Rev. mod. Phys.* **25** (1953) 831.
6. Munn, R. J., Smith, F. J., Mason, E. A. and Monchick, L., *J. chem. Phys.* **42** (1965) 537.
7. Mason, E. A., *J. chem. Phys.* **22** (1954) 169.
8. Loschmidt, J., *Sitzungsber. Akad. Wiss. Wien* **61** (1870) 367.
9. Ney, E. P. and Armistead, F. C., *Phys. Rev.* **71** (1947) 14.
10. Schmidt, R., *Ann. Physik* **14** (1904) 801; Lonius, A., *Ann. Physik* **29** (1909) 664.
11. Strehlow, R. A., *J. chem. Phys.* **21** (1953) 2101.
12. Amdur, I. and Schatzki, T. F., *J. chem. Phys.* **27** (1957) 1049; **29** (1958) 1425.
13. Ivakin, B. A. and Suetin, P. E., *Zhur. Tek. Fiz.* **34** (1964) 1115.
14. Holsen, J. N. and Strunk, M. R., *I. and E.C. Fund.* **3** (1964) 143.
15. Freudenthal, J., *Proc. 7th Int. Conf. Phen. Ion. Gases* **1** (1966) 53 (Beograd); Hogervorst, W. and Freudenthal, J., to be published.
16. Schäfer, K. and Schuhmann, K., *Z. Elektrochem.* **61** (1957) 246.
17. Srivastava, B. N. and Srivastava, K. P., *J. chem. Phys.* **30** (1959) 984; Srivastava, K. P. and Barua, A. K., *Ind. J. Phys.* **33** (1959) 229; Srivastava, K. P., *Physica* **25** (1959) 571.
18. Golubev, I. F. and Bondarenko, A. G., *Gaz. Prom.* **8** (1963) 46.

- 19) Durbin, L. and Kobayashi, R., J. chem. Phys. **37** (1962) 1643.
- 20) Malinauskas, A. P., J. chem. Phys. **42** (1965) 156; **45** (1966) 4704.
- 21) Walker, R. E. and Westenberg, A. A., J. chem. Phys. **31** (1959) 519.
- 22) Giddings, J. C. and Seager, S. L., I. and E.C. Fund. **1** (1962) 277;  
Seager, S. L., Geertson, L. R. and Giddings, J. C., J. Chem. Eng. Data **8** (1963) 168.
- 23) Srivastava, B. N. and Paul, R., Physica **28** (1962) 646;  
Paul, R., Ind. J. Phys. **36** (1962) 464.
- 24) Watts, H., Trans. Far. Soc. **60** (1964) 1745; Canad. J. Chem. **43** (1965) 431.
- 25) Saxena, S. C. and Mason, E. A., Mol. Phys. **2** (1959) 379.
- 26) Klein, M., J. Res. Nat. Bur. Stand. **70A** (1966) 259.
- 27) Mason, E. A. and Rice, W. E., J. chem. Phys. **22** (1954) 522; 843.
- 28) Monchick, L., Mason, E. A., Munn, R. J. and Smith, F. J., Phys. Rev. **139** (1965) A 1076.
- 29) Boato, G. and Casanova, G., Physica **27** (1961) 571.
- 30) Saxena, S. C., Ind. J. Phys. **29** (1955) 587.
- 31) Gibert, R. and Dognin, A., C.R. **246** (1958) 2607.
- 32) Mason, E. A., J. chem. Phys. **32** (1960) 1832.
- 33) Barua, A. K. and Chakraborti, P. K., Physica **27** (1961) 753.
- 34) Clifton, D. G., J. chem. Phys. **38** (1963) 1123.
- 35) Chakraborti, P. K., Physica **29** (1963) 227.
- 36) Zener, C., Phys. Rev. **37** (1931) 556.
- 37) Kilpatrick, J. E., Keller, W. E. and Hammel, E. F., Phys. Rev. **97** (1955) 9.
- 38) Corner, J., Trans. Far. Soc. **44** (1948) 914.
- 39) Srivastava, K. P., Ind. J. Phys. **31** (1957) 404.
- 40) Nicholson, G. A. and Schneider, W. G., Canad. J. Chem. **33** (1955) 589.
- 41) Saxena, S. C., Kelly, J. G. and Watson, W. W., Phys. Fluids **4** (1961) 1216.
- 42) Madan, M. P., J. chem. Phys. **23** (1955) 763; **27** (1957) 113.
- 43) Whalley, E. and Schneider, W. G., J. chem. Phys. **23** (1955) 1644.
- 44) Paul, R., Howard, A. J. and Watson, W. W., J. chem. Phys. **39** (1963) 3053; **43** (1965) 1890;  
Paul, R. and Watson, W. W., J. chem. Phys. **45** (1966) 4132.
- 45) Bernstein, R. B. and Muckerman, J. T., Advances in Chemical Physics (J. O. Hirschfelder, Ed., John Wiley and Sons, Inc., New York, 1967).

## SAMENVATTING

Uit het gedrag van de transportgrootheden in een binair mengsel van verdunde gassen kan men met behulp van de Chapman-Enskogtheorie informatie verkrijgen over de paarinteracties tussen twee ongelijksoortige moleculen. In het algemeen leveren, behalve de paarinteracties tussen ongelijksoortige moleculen, ook die tussen identieke moleculen een bijdrage tot het transport in mengsels, maar bij diffusie speelt de laatstgenoemde bijdragenage- noeg geen rol. De diffusiecoëfficiënt is daarom de meest directe bron van infor- matie over deze „meng“-interacties. In dit proefschrift is de diffusiecoëffi- ciënt van een aantal binaire mengsels nader bestudeerd. Het onderzoek heeft zich in hoofdzaak beperkt tot mengsels van edelgassen omdat men hiervoor kan verwachten dat de Chapman-Enskogtheorie toepasbaar is met ge- bruikmaking van een eenvoudig potentiaalmodel voor de paarinteracties, zoals de Lennard-Jones (12-6) potentiaal. Gegevens over de paarinter- acties kunnen dan worden verkregen in de vorm van numerieke waarden voor de karakteristieke parameters van deze potentiaal.

Informatie van betekenis over de potentiaalparameters kan men slechts verkrijgen indien men beschikt over nauwkeurige metingen van de diffusie- coëfficiënt in een groot en geschikt gekozen temperatuurgebied. Voor experi- menten met edelgasmengsels moet het temperatuurgebied zich voornamelijk beneden kamertemperatuur uitstrekken opdat de attracties tussen de mole- culen van voldoende betekenis zijn. Omdat er tot nu toe nagenoeg uitsluitend diffusieëxperimenten zijn gedaan rondom kamertemperatuur is in eerste in- stantie getracht de leemte in het lagere temperatuurgebied experimenteel op te vullen. Bovendien blijkt in het algemeen de nauwkeurigheid van bestaan- de experimenten dermate teleurstellend te zijn dat het noodzakelijk is der- gelijke metingen ook bij hogere temperatuur uit te voeren.

In hoofdstuk I wordt de methode beschreven die het mogelijk gemaakt heeft nauwkeurige metingen van de diffusiecoëfficiënt te verrichten in het temperatuurgebied tussen 65 en 295°K. De betrouwbaarheid van het appa- raat is uitvoerig onderzocht met het mengsel stikstof-waterstof. Zowel de

afhankelijkheid van de temperatuur als die van de concentratie blijkt zeer goed beschreven te worden door de Chapman-Enskogtheorie, gebruik makend van zowel de Lennard-Jones (12-6) potentiaal als de (exp-6) potentiaal voor de  $N_2-H_2$  wisselwerking. Uit de experimenten kan men voor beide modellen nauwkeurig een stel parameters bepalen.

In hoofdstuk II worden diffusiemetingen beschreven aan alle binaire mengsels van de edelgassen: He, Ne, Ar, Kr en Xe. De afhankelijkheid van de diffusiecoëfficiënt van temperatuur en concentratie is bepaald tussen 65 en  $400^\circ K$ . Evenals in hoofdstuk I kunnen in het algemeen de potentiaalparameters worden berekend voor diverse potentiaalmodellen. Dergelijke resultaten voor de meng-interacties heeft men niet eerder kunnen verkrijgen, noch uit diffusiemetingen noch uit andere bronnen. Alleen over de moleculaire wisselwerking in zuivere gassen bestaan voldoende gegevens. Het is daarom eerst nu goed mogelijk geworden de samenhang te onderzoeken tussen de paarinteracties van ongelijksoortige moleculen en die van gelijke moleculen in een mengsel. Voor het beschrijven van deze samenhang maakt men meestal gebruik van enige semi-empirische combinatieregels tussen de voorkomende potentiaalparameters. De geldigheid van deze regels is systematisch onderzocht in hoofdstuk II. Het blijkt dat de gebruikelijke combinatieregels niet voldoen.

In Polar, Drs. A. van Daelen en J. H. Halpe, die raad van de  
taal Drs. A. Feberwee mij veel steun gaf bij de scriptie over  
leid op betrouwbare resultaten in de bepalingen. Veel medewerking heb ik  
gekregen van de technische staf van het Kamerlingh Onnes Laboratorium,  
in het bijzonder van de heren H. R. A. Kater, J. M. Verbeek, A. K. H.  
Gevriss en J. Taconis onder wier leiding de apparatuur werd ver-  
vuldigd en van de heer W. F. Tackx die zorg droeg voor de laboringen.  
Mijn A. M. Achterhuis ik voor de snelle en accurate verzorging van het  
materiaal. Verder ben ik de heren Prof. Dr. R. A. Aals en Dr. T. K.  
Dose erkentelijk voor het lezen van het manuscript en het corrigeren van  
de drukke teksten. De Stichting F.O.M. ben ik dank verschuldigd voor het  
beschikbare stellen van het archief van publicaties voor dit proefschrift.

Teneinde te voldoen aan de wens van de Faculteit der Wis- en Natuurkunde volgt hier een overzicht van mijn universitaire studie.

Na in 1956 het eindexamen B te hebben afgelegd aan de R.K. H.B.S. van het St. Janscollege (thans lyceum) te 's-Gravenhage begon ik in oktober van hetzelfde jaar mijn studie aan de Rijksuniversiteit te Leiden. Het candidaatsexamen natuurkunde en wiskunde, bijvak scheikunde, legde ik af in oktober 1959. Sindsdien was ik werkzaam op het Kamerlingh Onnes Laboratorium in de molecuulfysicagroep onder leiding van Prof. Dr. K. W. Taconis en Prof. Dr. J. J. M. Beenakker. Mijn inwijding in deze tak van fysica heb ik voornamelijk te danken aan Dr. C. M. Knobler onder wiens leiding ik deelnam aan experimenten over mengwarmte en magnetische susceptibiliteit van de vloeistofsystemen zuurstof-stikstof en zuurstof-argon. Daarnaast werkte ik enige tijd aan röntgendiffractie in vloeibare zuurstof. Vervolgens assisteerde ik Dr. H. F. P. Knaap bij zijn onderzoek aan de mengwarmte van isotopen van vloeibare waterstof. Het doctoraal examen in de experimentele natuurkunde met mechanica legde ik af in oktober 1962. Sindsdien zette ik het werk voort van Drs. F. A. Bottemanne aan diffusie hetgeen uiteindelijk resulteerde in dit proefschrift.

Sedert 1960 ben ik verbonden aan de Stichting voor Fundamenteel Onderzoek der Materie (F.O.M.), waarvan in het tijdvak voor mijn doctoraal examen in de functie van wetenschappelijk medewerker met studietoelage en daarna als wetenschappelijk medewerker in gewoon verband. Het in dit proefschrift beschreven onderzoek werd uitgevoerd als onderdeel van het programma van de werkgroep F.O.M. M II en is mogelijk gemaakt door subsidie van de Nederlandse Organisatie voor Zuiver Wetenschappelijk Onderzoek (Z.W.O.).

Veel steun heb ik ondervonden van de efficiënte discussies met Dr. H. F. P. Knaap. De adviezen van Prof. Dr. K. W. Taconis en Dr. C. J. N. van den Meijdenberg waren zeer waardevol. Bij mijn onderzoek werd ik achtereenvolgens geassisteerd door de heren Drs. A. Feberwee, Drs. P.

L. Polak, Drs. A. van Oosten en J. P. Harpe, ph. cand., van wie speciaal Drs. A. Feberwee mij veel steun gaf bij de schijnbare uitzichtloosheid op betrouwbare resultaten in de beginperiode. Veel medewerking heb ik gehad van de technische staf van het Kamerlingh Onnes Laboratorium, in het bijzonder van de heren H. R. A. Nater, J. M. Verbeek, A. R. B. Gerritse en J. Turenhout onder wier leiding de apparatuur werd vervaardigd, en van de heer W. F. Tegelaar die zorg droeg voor de tekeningen. Mej. A. M. Aschoff dank ik voor de snelle en accurate verzorging van het manuscript. Verder ben ik de heren Prof. Dr. R. A. Aziz en Dr. T. K. Bose erkentelijk voor het lezen van het manuscript en het corrigeren van de Engelse tekst. De Stichting Physica ben ik dank verschuldigd voor het beschikbaar stellen van het zetsel van publikaties voor dit proefschrift.



## STELLINGEN

### I

De nauwkeurigheid van de algemeen gebruikte combinatie-regels tussen de parameters, die de verschillende soorten piekinteracties in een binair mengsel karakteriseren, is waarschijnlijk geringer dan men veelal veronderstelt.

Zie postscript, hoofdstuk II.

### II

Greere's act en verwachte gedrag van de diffusiecoëfficiënt als functie van de concentratie van de binaire mengsels van helium met de andere edelgassen is het interessant voor dezelfde mengsels ook thermodynamische experimenten uit te voeren.

Zie postscript, hoofdstuk II.

### III

De viscositeitscoëfficiënten van heliumgas, zoals die experimenteel bepaald zijn door Gurevants *et al.* bij lage temperaturen en door Johnston *et al.*, of Truax *et al.* bij hogere temperaturen, zijn niet met elkaar in overeenstemming te brengen naar gebruik te maken van de Chapman-Enskogtheorie met een redelijke potentiële dan het (exp-6) model.

T. M. J. Gurevants, N. van Lierhoek, J. J. M. Baenaeker, H. E. D. Knapp en P. Zandbergen, *Physica* 24 (1954) 537.

H. L. Johnston en R. W. Griggs, *J. phys. Chem.* 46 (1942) 762.

M. Truax en R. Zink, *Ann. Physik* 7 (1928) 427.

### IV

Volgens Herzfeld en Litavitz gedraagt de reciproke waarde van de afwezigheidsrelaxatietijd in binair mengsel van een relaxerend gas met een edelgas zich lineair in de concentratie. Afwijkingen van dit gedrag kunnen echter worden verwacht in waterstof-xenon mengsels met lage waterstofconcentratie.

R. F. Herzfeld en T. A. Litavitz, "Absorption and Dispersion of Ultrasound Waves" (Academic Press, New York, 1957).

L. Potak, Drs. A. van Gesten en J. B. Harpe, ph. cand., van wie speciaal Drs. A. Faber mee mij veel steun gaf bij de schijnbare nitricheid op betrouwbare resultaten in de beginperiode. Veel medewerking heb ik gehad van de technische staf van het Koninklijk Onderzoekslaboratorium, in het bijzonder van de heren H. R. A. Nater, J. M. Verbeek, A. R. B. Geelkes en J. Torenhoof onder wier leiding de apparatuur werd vervaardigd, en van de heer W. F. Tegelaar die zorg droeg voor de tekeningen. Mej. A. M. Aschoff dank ik voor de snelle en accurate verzorging van het manuscript. Verder ben ik de heren Prof. Dr. R. A. Astz en Dr. T. K. Bose erkentelijk voor het lezen van het manuscript en het corrigeren van de Engelse tekst. De Stichting Physica ben ik dank verschuldigd voor het beschikbaar stellen van het fonds van publicaties voor dit proefschrift.

## STELLINGEN

### I

De nauwkeurigheid van de algemeen gebruikte combinatieregels tussen de parameters, die de verschillende soorten paarinteracties in een binair gasmengsel karakteriseren, is aanzienlijk geringer dan men veelal veronderstelt.

Dit proefschrift, hoofdstuk II.

### II

Gezien het onverwachte gedrag van de diffusiecoëfficiënt als functie van de concentratie van de binaire mengsels van helium met de andere edelgassen is het interessant voor dezelfde mengsels ook thermodiffusie-experimenten uit te voeren.

Dit proefschrift, hoofdstuk II.

### III

De viscositeitscoëfficiënten van heliumgas, zoals die experimenteel bepaald zijn door Coremans e.a. bij lage temperaturen en door Johnston e.a. of Trautz e.a. bij hogere temperaturen, zijn niet met elkaar in overeenstemming te brengen door gebruik te maken van de Chapman-Enskogtheorie met een realistisch potentiaal dan het (exp-6) model.

J. M. J. Coremans, A. van Itterbeek, J. J. M. Beenakker, H. F. P. Knaap en P. Zandbergen, *Physica* **24** (1958) 557.

H. L. Johnston en E. R. Grilly, *J. phys. Chem.* **46** (1942) 948.

M. Trautz en R. Zink, *Ann. Physik* **7** (1930) 427.

### IV

Volgens Herzfeld en Litovitz gedraagt de reciproke waarde van de akoestische relaxatietijd in binaire mengsels van een relaxerend gas met een edelgas zich lineair in de concentratie. Afwijkingen van dit gedrag kunnen echter worden verwacht in waterstof-xenon mengsels met lage waterstofconcentratie.

K. F. Herzfeld en T. A. Litovitz, "Absorption and Dispersion of Ultrasonic Waves" (Academic Press, New York, 1959).

## STELLINGEN

### I

De nauwkeurigheid van de algemeen gebruikte combi-stempels tussen de parameters die de verschillende soorten partitietacties in een binair gas-mengsel karakteriseren, is aanzienlijk geringer dan men verdedigen zoude.

De presentatie, hoofdstuk II.

### II

Lezen het onverwachte gedrag van de diffusiecoëfficiënt als functie van de concentratie van de binaire mengsels van belang met de andere gegevens is het interessant voor dezelfde mengsels ook thermodynamische experimenten uit te voeren.

De presentatie, hoofdstuk II.

### III

De verscheidenheid van de diffusiecoëfficiënten van oplossingen, zoals die experimenteel bepaald zijn door Correns en bij hoge temperaturen en door Johnson en de Franke en bij lagere temperaturen, zijn niet met elkaar in overeenstemming te brengen door gebruik te maken van de Chapman-Enskogtheorie met een verbeterde potentiaal dan het (exp-6) model.

J. M. J. Correns, A. van der Hoff, J. M. H. Franke, M. E. P. Knaap en F. Xandbergen, *Tijdschr. v. d. Chem.* 24 (1956) 583.  
H. J. Johnson en H. H. Gilroy, *J. Phys. Chem.* 64 (1960) 768.  
M. Franke en H. Xandbergen, *Tijdschr. v. d. Chem.* 24 (1956) 457.

### IV

Volgens Herzfeld en Litovitz wijst de wetmatige waarde van de absolute relaxatietijd in binaire mengsels van een niet-rekend gas met een enkelvoudig gas naar de concentratie. Afwijkingen van dit gedrag kunnen echter worden verwacht in waterstof-water mengsels met lage waterstofconcentraties.

H. N. Herzfeld en T. A. Litovitz, "Absorption and Dispersion of Ultrasound Waves", Academic Press, New York, 1959.

## V

De experimenten van Sahri aan gedeuteerd cobaltchloridehexahydraat vormen nog geen overtuigend bewijs dat waterstofbruggen een essentiële rol spelen bij het superexchange-mechanisme in dit kristal.

D. S. Sahri, *Phys. Letters* **19** (1966) 625.

## VI

Bij het berekenen van het maximum veld dat door een condensatorontlading in een pulsmagneet geproduceerd kan worden, is het nodig de opwarming van de magneetspoel in aanmerking te nemen.

Y. Allain, F. Varret en A. Miédan-Gros, *C.R.* **260** (1965) 4677.

## VII

Gezien de ervaringen opgedaan bij omgekeerde osmose door poreuze cellulose-acetaatmembranen lijkt het resultaat van Morgan e.a., dat totale retentie van organische stoffen bij dit proces optreedt, onwaarschijnlijk.

S. Sourirajan, *I.&E.C. Product Research and Development* **4** (1965) 201.

A. I. Morgan, Jr., E. Lowe, R. L. Merson en E. L. Durkee, *Food Tech.* (Dec. 1965) **52** (1790).

## VIII

Het principiële verschil in constructie tussen een brander voor aardgas en een voor stadsgas mag zich slechts uiten in de vlamstabilisatie.

## IX

Het heeft weinig zin ter vermindering van staande trillingen in een luidsprekerbehuizing langs de wanden geluidsabsorberend materiaal aan te brengen.

## X

Bij het streven naar verkorting van de studieduur aan universiteiten moet men bedenken dat lijfstraffen eerder een gunstige invloed kunnen hebben dan een verlichting van de exameneisen.

## XI

In vrijwel alle in de fotografie voorkomende gevallen biedt de reflex-camera belangrijke voordelen boven de meetzoekercamera.



